OPTIMIZATION OF MINE VENTILATION FAN SPEEDS ACCORDING TO VENTILATION ON DEMAND AND TIME OF USE TARIFF

by

Arnab Chatterjee

Submitted in partial fulfillment of the requirements for the degree

Master of Engineering (Electrical Engineering)

in the

Department of Electrical, Electronic and Computer Engineering
Faculty of Engineering, Built Environment and Information Technology
UNIVERSITY OF PRETORIA

September 2014

SUMMARY

OPTIMIZATION OF MINE VENTILATION FAN SPEEDS ACCORDING TO VENTILATION ON DEMAND AND TIME OF USE TARIFF

by

Arnab Chatterjee

Supervisor(s):	Prof X. Xia
Department:	Electrical, Electronic and Computer Engineering
University:	University of Pretoria
Degree:	Master of Engineering (Electrical Engineering)
Keywords:	Energy efficiency, load management, mine ventilation, optimization, time of use tariff, ventilation on demand (VOD).

With the growing concerns about energy shortage and demand supply imbalance, demand side management (DSM) activities has found its way into the mining industry. This study analyzes the potential to save energy and energy-costs in underground mine ventilation networks, by application of DSM techniques. Energy saving is achieved by optimally adjusting the speed of the main fan to match the time-varying flow demand in the network, which is known as ventilation on demand (VOD). Further cost saving is achieved by shifting load to off-peak or standard times according to a time of use (TOU) tariff, i.e. finding the optimal mining schedule.

The network is modelled using graph theory and Kirchhoff's laws; which is used to form a non-linear, constrained, optimization problem. The objective of this problem is formulated to minimize the energy cost; and hence it is directly given as a function of the fan speed, which is the control variable. As such, the operating point is found for every change in the fan speed, by incorporating the fan laws and the system curve.

The problem is solved using the *fmincon* solver in Matlab's optimization toolbox. The model is analyzed for different scenarios, including varying the flow rate requirements and

tariff structure. Although the results are preliminary and very case specific, the study suggests that significant energy and energy-cost saving can be achieved in a financially viable manner.

OPSOMMING

SPOED OPTIMERING VAN VENTILASIE WAAIERS IN MYNE VOLGENS VENTILASIE-OP-AANVRAAG EN TYD-VAN-VERBRUIK TARIEWE

deur

Arnab Chatterjee

Studieleier(s):	Prof X. Xia
Departement:	Elektriese, Elektroniese en Rekenaar-Ingenieurswese
Universiteit:	Universiteit van Pretoria
Graad:	Magister in Ingenieurswese (Elektriese Ingenieurswese)
Sleutelwoorde:	Energie-doeltreffendheid, aanvragbestuur, myn ventilasie, optimering, tyd-van-vebruik tariewe, ventilasie-op-aanvraag.

Die fokus op die bestuur van energieverbruik kom nou ook in die mynbedryf voor. Dié studie analiseer die potensiaal om energie te bespaar en sodoende energie kostes te verminder deur die toepassing van energie aanvraagbestuur tegnieke. Energiebesparing is moontlik deur die verandering van die hoofwaaiers in myne se spoed aan te pas met die tydveranderlike vloei van die ventilasie netwerk, wat bekend staan as ventilasie-op-aanvraag. Verdere energiekoste besparing is moontlik deur die verskuiwing van energieverbruik tot buite piektyd volgens tyd van vebruik tariewe.

Die ventilasie netwerk word gemodelleer deur middel van grafiekteorie en Kirchoff se wette. Hierdie wette is gebruik om 'n nie-lineêre, beperkte optimering probleem te formuleer. Die doelwit van die probleem is om energiekostes te minimeer. Die probleem word gestel as 'n funksie van waaier spoed, wat die beheerde veranderlike is. 'n Bedryfspunt word bepaal vir elke verandering in waaierspoed deur die gebruik van waaierwette en ventilasie stelsel kurwes.

Die probleem word opgelos deur Matlab se *fmincon* funksie in die Matlab *Optimization Toolbox*. Die model word geanaliseer vir verskeie moontlikhede insluitend die verandering van vloeitempobehoeftes of die verandering van tariefstrukture. Alhoewel die resultate voorlopig

en geval-spesifiek is, bewys die studie dat merkwaardige energie en energiekoste besparing moontlik is op 'n manier wat finansieël sin maak.

LIST OF ABBREVIATIONS

DSM	Demand side management
EE	Energy efficiency
GA	Genetic algorithm
HVAC	Heating, ventilation, and air conditioning
KCL	Kirchoff's current law
KVL	Kirchoff's voltage law
LM	Load management
OEL	Occupational Exposure Limit
PI	Post implementation
RPM	Rotations per minute
RTP	Real time pricing
SQP	Sequential quadratic programming
TOU	Time of use
VOD	Ventilation on demand
VSD	Variable speed drive

TABLE OF CONTENTS

CHAPTER 1

INTRODUCTION

1.1 PROBLEM STATEMENT

Energy is an essential requirement for economic growth and sustainability of a country. With an ever increasing demand for energy around the world, suppliers are struggling to keep up. This is no different for South Africa. The main reason behind the current energy crisis in the country is due to the fact that Eskom (the national electricity utility) is struggling to supply enough power to match the demand. Therefore there exists two solutions for this problem, i.e. either increase supply or decrease demand. Eskom has already started work to expand their supplying capacity. This is, however, a long term plan and the short term issue is being addressed via Eskom's Demand Side Management (DSM) programme. This programme seeks to reduce the gap between supply and demand by mainly two approaches, viz. Energy Efficiency (EE) and Load Management (LM). The LM approach aims to reduce electricity demand at peak periods by shifting load to off-peak and standard periods; and the EE approach aims to reduce overall electricity consumption by installing energy efficient equipment and optimizing industrial processes [1].

It is known that the industrial sector consumes about 37% of the world's total delivered energy, and out of this, the mining industry contributes about 9% [2]. Comparatively, in South Africa, the industrial sector is responsible for about 41% of the total national energy demand; and due to the economy being structured around energy intensive mining and minerals industries, the mining and quarrying sub-sector makes up 16% of the total energy consumed by the industrial sector [3]. Thus, the mining industry is identified as a potential target to investigate energy saving opportunities, by application of DSM techniques.

Mine ventilation is a crucial part of safety in mines, because it is responsible for clearing out noxious and flammable gasses. Apart from this, it also provides a comfortable working environment underground. Since the source of the air flow is controlled by fans, there is an associated cost of energy. The rating of the fans, depending on its use, usually range from 100 kW [4, 5] to about 3000 kW [6, 7]. The auxiliary fans are usually the lower rated ones, whereas the main fans are usually rated higher. When taking into account the contribution of power consumption by the ventilation fans towards the total power consumption, the result can be quite significant. Research suggests that, depending on the type of mine, ventilation underground can consume between 20% and 40% of the total electricity used by the mine [8, 9]; and up to 60% [10] of mining operating cost can be attributed to ventilation underground. Thus, the concept of ventilation on demand (VOD) is explored. This technique involves varying fan speeds, in order to supply a time varying demand.

The work presented in this dissertation focuses on finding the possible energy and energy-cost savings in an underground mine ventilation network. These savings can be achieved by adjusting the speed of the main fan, via a VSD, such that it adheres to a VOD profile.

1.2 RESEARCH OBJECTIVE AND QUESTIONS

The objective of this study is to develop an optimization model for an underground mine ventilation network that can find the maximum possible energy and cost saving. This is achieved by considering an EE method, i.e. implementing VSDs to vary the fan speed and finding an optimal speed profile; and by applying an LM technique, i.e. optimally shifting load to off-peak and standard times according to the TOU tariff.

The following research questions are put forward, relative to this objective:

- How does extending the existing models, for optimizing the flow distribution in a ventilation network, change the results?
- How does the application of VSDs to mine ventilation compare to other similar research?
- How does cost saving perform when comparing EE to LM?
- What factors affect the energy and cost savings?

- What is the economic feasibility of performing these DSM activities?

1.3 HYPOTHESIS AND APPROACH

It is hypothesized that by controlling the speed of the main fan in a mine, the energy consumption and the energy costs associated with it can be reduced. To test this hypothesis, the following sequential approach is followed:

1. Literature study - Background on ventilation networks and fans must be studied, in order to understand the existing models.

2. Modelling - A generic mathematical optimization model must be developed.

3. Results - An algorithm must be selected to solve the optimization problem. A case study must be considered to test the model, and obtain results.

4. Analysis - The results obtained from solving the optimization problem must be analyzed to answer the research questions.

1.4 RESEARCH CONTRIBUTION

The use of VSDs is becoming very popular in industrial applications as a method of reducing energy and related costs. However, from a research perspective, controlling the main fan in mines has not been largely explored. Thus this study will present a generic model that can be applied to a mine ventilation network, in order to find the optimal speed profile of the main fan. This research can provide an academic foundation for decision making, regarding installing VSDs on main fans in mines around the world. It is of particular interest to the South African economy, given how energy intensive the country is.

1.5 CHAPTER SUMMARY

This study addresses the short term solution of the current energy crisis. The research objectives involve the use of DSM strategies, applied to underground mining ventilation networks. The contribution of the study focuses on finding the optimal speed profile of the main mine fan.

CHAPTER 2

LITERATURE STUDY

This chapter presents the literature that was required in order to conduct this research and is necessary to achieve the research objectives. Thus DSM was studied, along with its current application to industries; this included application of VSDs. A review on mine ventilation was also done, with focus on existing strategies to reduce costs, and mathematical modelling of the network.

2.1 DEMAND SIDE MANAGEMENT

2.1.1 Description

The traditional concept of managing supply and demand for power has been: if society demands more power, the utility will generate more to supply it, even if it means building new generation units. This is known as supply side management [11, 12]. This however is a long term plan, because building of generation units take a long time compared to the rate at which demand might increase. Thus, DSM programmes are being introduced worldwide, as a cost effective and short term method to maintain the required margin between supply and demand.

The concept of DSM has been around for over 4 decades. Though not technically defined then, literature suggests that the process of clipping peak load and load shifting existed in New Zealand and Europe as far back as the 1960's [1]. It wasn't until the late 70's, however, that the concept of DSM began to appear in technical articles and even later in academic research. This was mainly prompted by the oil embargo in the 1970's, which caused oil

prices to increase rapidly [13, 14]. Due to the markets around the world being liberalized and deregulated during the 90's, many utilities lost interest in DSM, as they had to compete for electricity supply and thus perceived DSM to be unprofitable [15, 13, 16]. However, since the 2000's focus had shifted in government policies towards climate change and energy security, which, again, encouraged research in the field of DSM [15, 17].

The definition of DSM has many variations throughout literature. However, most definitions tend to lead towards manipulating the end user's electricity usage pattern, in order to maintain a safe margin between supply and demand. The earliest traceable definition was published by Gellings [1], which many succeeding articles seem to cite. Gellings said that "DSM is the planning, implementation, and monitoring of those utility activities designed to influence customer use of electricity in ways that will produce desired changes in the utility's load shape". Classic techniques of DSM include [1, 16, 12, 17]:

- Peak clipping - This process involves cutting load during times when demand is the highest, and avoiding the use of expensive generation. The utility may have direct control over the end user's appliances, or the customer can implement this by himself as well. An illustrative example is shown in fig. 2.1.

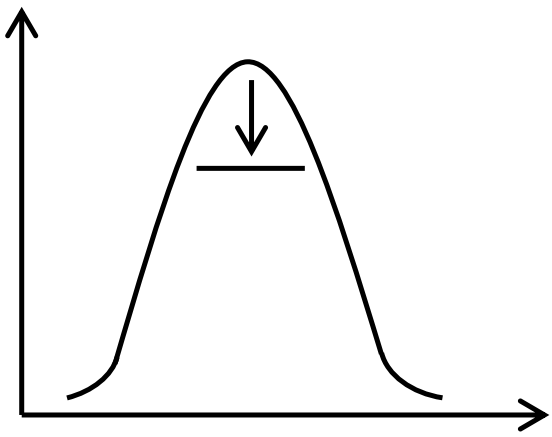

Figure 2.1: Illustration of peak clipping

- Valley filling - This process encourages customers to increase energy usage during off-peak periods, such that a better load factor is achieved, which is beneficial to the utility and the average customer. An illustrative example is shown in fig. 2.2.

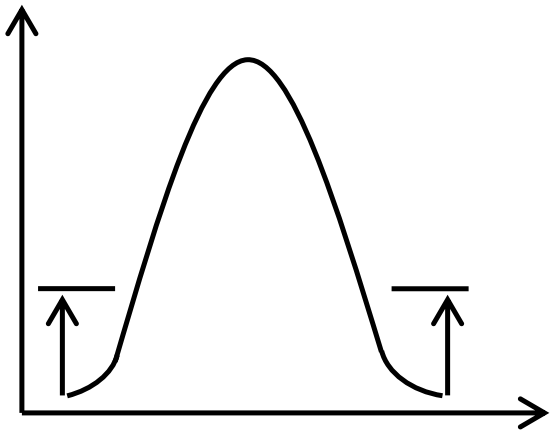

Figure 2.2: Illustration of valley filling

- Load shifting - This process entails shifting load from more expensive periods to cheaper periods, i.e. it is a combination of peak clipping and valley filling, and thus the benefits from both the processes are obtained. An illustrative example is shown in fig. 2.3.

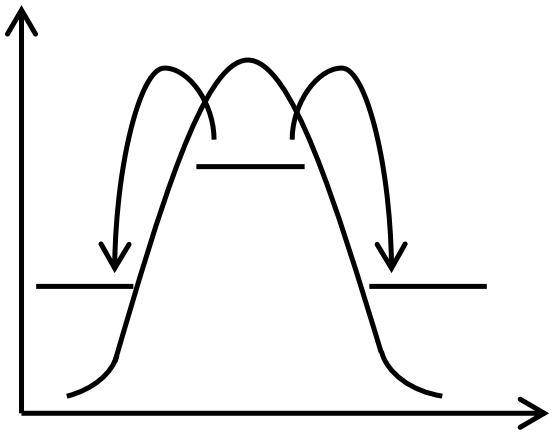

Figure 2.3: Illustration of load shifting

- Strategic conservation - This is the process of reducing overall demand, regardless of the time of day. This can postpone the need for extra capacity. An illustrative example is shown in fig. 2.4.

- Strategic load growth - Much like valley filling, this process encourages users to increase energy consumption, but at any time. This occurs when there is excess capacity available and/or there are areas of community without electricity. This also promotes the

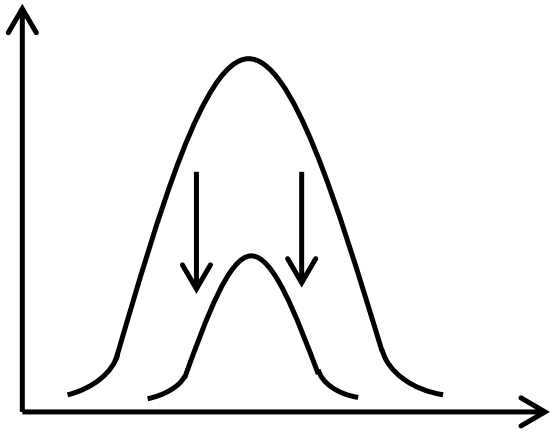

Figure 2.4: Illustration of strategic conservation

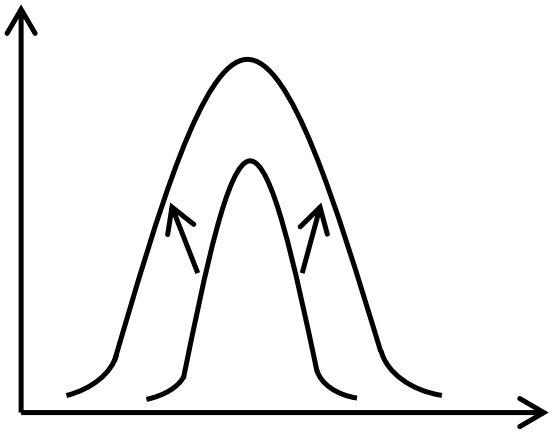

Figure 2.5: Illustration of strategic load growth

use of renewable sources and greener technologies. An illustrative example is shown in fig. 2.5.

As the world moves towards a more 'greener' society, the definition of DSM has slightly changed. With growing concerns about the environment and energy security, energy is definitely climbing the political agenda. As such, newer approaches towards DSM would typically exclude the valley filling and strategic load growth options from the acceptable techniques. Thus, a more recent definition, as described by Warren [15] would be, "DSM refers to technologies, actions and programmes on the demand-side of energy metres that seek to manage or decrease energy consumption, in order to reduce total energy system expenditures or contribute to the achievement of policy objectives such as emissions reduction or balancing

supply and demand."

Within this definition, two major categories are encompassed as discussed below.

1. Energy Efficiency - The aim is to reduce overall energy demand.

    - Efficiency - This is defined as the ratio of useful output of a process to its energy input [18]. Thus using less energy to produce the same output is what is required, as opposed to increasing the output while using the same amount of energy (which would also be considered an efficiency improvement, by definition). The most popular techniques to achieve this include: using more efficient technologies in lighting, using more efficient techniques and fuel switching in the HVAC environment, using more efficient motors and the use of VSDs on motors [12, 14].

    - Conservation - This is defined as an overall energy demand reduction in a year [15]. This can be achieved mainly by changes in behavioural or usage patterns, e.g. reducing consumption of hot water; switching off lights, fans, and other equipment when not required; maximizing use of natural heat, light, and ventilation.

2. Demand-Side Response - The aim is to reduce demand at peak times.

    - Price Based [11, 19] - This is a technique where the cost of electricity is determined by the usage pattern of the consumer. E.g. TOU tariffs define a set of prices that are higher during peak times of the day, compared to off-peak periods; RTP is more dynamic, and involves tariff changes based on the market price; and a maximum demand charge is billed on top of the normal energy charge, according to the maximum demand (in kVA) across a set period. These techniques encourage customers to either shift load from peak times or clip the peaks, in order to reduce their electricity bills.

    - Incentive Based [11, 19] - This technique requires a contractual agreement between the utility and the customer. It involves the customer receiving payment to voluntarily curtail load. The load can be directly cut by the utility at a pre-determined time, which is known as direct control; or the customer can have the option of curtailing load during that time, which is known as indirect control. The pricing

strategies obviously differ for these 2 cases, and is another scope of research by itself.

2.1.2 DSM applications

DSM techniques are applied in various industries as can be found in literature. Some applications consider load shifting by finding the optimal switching times of equipment according to the TOU tariff. This includes controlling of conveyor belts, e.g., [20] shows that a 49% cost saving is possible by controlling the conveyor belts in a colliery; whereas [21] shows a 28.3% cost saving at a coal fired power plant. Switching of pumps is also common, e.g., [22] shows that it is possible to save up to 5.8% of energy related costs in a water purification plant; and [23] suggests a maximum cost saving of 32% at a pumping station. Another study showed that by controlling a residential hot water geyser, cost savings of up to 35% is possible [24]. Also, [25] shows how it is possible to control various equipment as part of a batch process in a steel plant, to save about 5.7% in electricity costs. These examples show significant cost saving compared to the baseline case, but actual energy saving is very little because the objective is focused on load shifting from peak periods.

Considerable attention has also been drawn to EE improvement of industrial processes by the application of VSDs. In particular, the application of VSDs to fans and pumps have been studied, reasons being that VSDs offer more energy saving than a simple switching strategy [21, 26] and a small reduction in the speed can result in large energy savings [27, 28, 29]. E.g. in [26], it is shown that there is potential to save up to 45% of electrical energy in a greenhouse and poultry house, if the fan speed is adjusted via a VSD. Reference [30] showed that VSD application to pumps, used in cooling underground mines, can save about 30% electricity. Another example is shown in [31], where varying the speed of the fan in a boiler house, used to supply the air for combustion, can save up to 34% electricity. However, these examples don't consider LM under the TOU tariff in order to shift load from peak time.

Only [32] considers achieving both EE and LM. It considers switching and the application of a VSD simultaneously, to find the optimal balance between LS and EE.

2.2 MINING VENTILATION

2.2.1 Ventilation requirements

Mining ventilation can be described as the use of scientific principles to perform activities in underground mines, to provide and maintain a safe, healthy, and comfortable working environment. This is done by meeting the following basic requirements [33, 34]:

1. Supply oxygen for breathing, which must be between 19% and 19.5% by volume. It is shown that oxygen levels below this value can have negative effects on the health of a mine worker.

2. Remove heat, i.e. cool the surrounding temperatures to provide a comfortable working environment, which can affect production. Only ventilation is often not enough for cooling purposes, and thus cool water and chillers are often part of the system.

3. Dilute and remove toxic and explosive gases from working environments.

4. Dilute and remove hazardous airborne pollutants from working environments.

The ventilation requirements, in terms of the airflow rates, are usually determined by the engineers based on respiratory, health, safety and operation requirements set by the local mining governing body. The legal requirements are often given in terms of their Occupational Exposure Limits (OEL's); e.g. table 2.1 shows the OEL's of some common gases in South African mines [33].

Table 2.1: OEL of common gases

Gas	OEL value (%)
Carbon dioxide (CO_2)	0.5
Carbon monoxide (CO)	0.0025
Nitrous fumes (NO_x)	0.0003
Hydrogen sulphide (H_2S)	0.0010
Ammonia (NH_3)	0.0025
Methane (CH_4)	1.4

Thus using such information, engineers can use mass flow and concentration equations to calculate the required flow rate based on the activity taking place. Apart from the flow rate calculation based on the gas and dust concentration limits, the total installed diesel power and the rock temperatures underground also feature in calculating the required flow rates. Typical flow rate values are shown below [34]:

- Fumes released by diesel equipment has to be removed. Flow rates was found to vary between 0.06 m^3/s and 0.09 m^3/s, per kW of installed diesel capacity.
- In order to meet the respiratory requirement of at least 19.5% O_2 and at most 0.5% CO_2, a flow rate of 0.01 m^3/s per person is required.
- To prevent methane build up, a minimum velocity of 0.25 m/s is required at all working areas. For a typical area of 6×2 metres, the minimum requirement works out to be 4 m^3/s.

Thus the design engineer must calculate the volumetric flow rate in each area of the mine, keeping in mind all the requirements discussed above.

2.2.2 Frictional losses of fluid flow

When considering airflow through a mine opening, it could be laminar, turbulent, or transitional in nature. Laminar flow can be described as the air particles moving smoothly in one direction, without mixing. Laminar flow often takes place at low flow velocities, and it is not capable of mixing with contaminant gases to dilute the air. In turbulent flow, the air flows in a specific direction, but within this flow, the motion of the particles are irregular and can differ in direction and velocity. Thus, turbulent flow is capable of mixing with the contaminant gases to dilute them. The transitional state falls in between the two extremes, thus containing sum turbulent flow, within laminar flow. The state of flow of a fluid depends on the Reynolds number, which is calculated based on the velocity of the fluid, the viscosity of the fluid, and the dimensions of the duct in which it is flowing. It is known from [35, 34] that the flow is considered to be laminar if the resulting Reynolds number is less than 2000; turbulent when the number is greater than 4000; and transitional for any number in between.

The Darcy-Weisbach equation, given below [35], is used to calculate the head losses in a pipe as function of the fluid velocity, due to friction.

$$h_f = \frac{\lambda v^2 L}{2gD}, \tag{2.1}$$

where h_f is the head loss due to friction, L is the length of the pipe, D is the hydraulic diameter of the fluid, v is the velocity of the pipe, g is the acceleration due to gravity, and λ is the Darcy friction factor.

For laminar flows, the friction factor is a direct function of the Reynolds number. However, to determine the friction factor for turbulent flows, either the Colebrook-White equation must be solved or Moody diagrams have to be used.

Based on eq. (2.1), Atkinson further developed an equation for the pressure loss in mine airways, due to friction. The derivation is as follows:

1. In order to convert the head loss (m) into a pressure loss (Pa) form, eq. 2.1 is multiplied by the density (ρ) and the acceleration of gravity (g).

2. The velocity, v, is replaced by the ratio of the flow rate to cross-sectional area, Q/A.

3. The hydraulic diameter is replaced by its fundamental formula, $D = 4A/P$, where P is the wetted perimeter of the cross-section.

4. This leads to the Atkinson Equation [34]:

$$\Delta p = \frac{1}{2}\rho \frac{\lambda L P Q^2}{4A^3}. \tag{2.2}$$

   The Atkinson resistance is defined as

$$R = k\frac{LP}{A^3}, \tag{2.3}$$

   where k, defined as the atkinson friction factor, is given by

$$k = \frac{1}{2}\rho\frac{\lambda}{4}. \tag{2.4}$$

2.2.3 Network analysis

Fresh air enters a mine through a downcast shaft. It is drawn through the working places, where it gets contaminated. It is then removed from the mine via the upcast shaft. The main fan can be situated in either the downcast shaft, the upcast shaft, or both. If the fan is situated in the downcast shaft, the system is known as a blower system. The fan pushes air into the mine and creates a higher air pressure inside than the atmospheric pressure outside. If the fan is located in the upcast shaft, the system is called an exhaust system. In this case, the fan sucks air out of the mine and a lower air pressure is created inside the mine, compared to the atmospheric pressure outside (see fig. 2.6). In some cases, where it is necessary to overcome high mine resistance, the blower and exhaust systems are combined to form a push and pull system.

The mine ventilation system can be divided into two basic components: primary ventilation and secondary (auxiliary) ventilation. The primary ventilation system focuses on the airflow through the network, and the secondary system deals with the airflow required for dead ends. Thus a booster fan would typically be installed in the primary route, whereas an auxiliary fan is used to supply air, via ducts, to a dead end or development end [36]. The primary ventilation system is less dynamic, in terms of ventilation requirements, compared to the auxiliary system. The auxiliary, or secondary, ventilation system is more dynamic because it is directly supplying the development ends, whose working conditions are changing frequently.

A mine is divided into various sections. To distribute and control the air amongst the various sections, ventilation appliances such as ventilation doors, walls, regulators, booster fans and auxiliary fans are used. Once the air enters underground through the downcast shaft, it needs to be distributed throughout the various air passages that link the working faces. These passages can be represented by a network with the help of graph theory.

The graph of a network is diagram that shows its structure. It consists of branches and nodes. For a ventilation network the branches represent the airways, through which the ventilation air flows; and the nodes represent the connection point of two or more branches. Thus a ventilation network can be represented by a directed and connected graph; this means that the direction of airflow is assumed (directed), and it is possible to move between any two

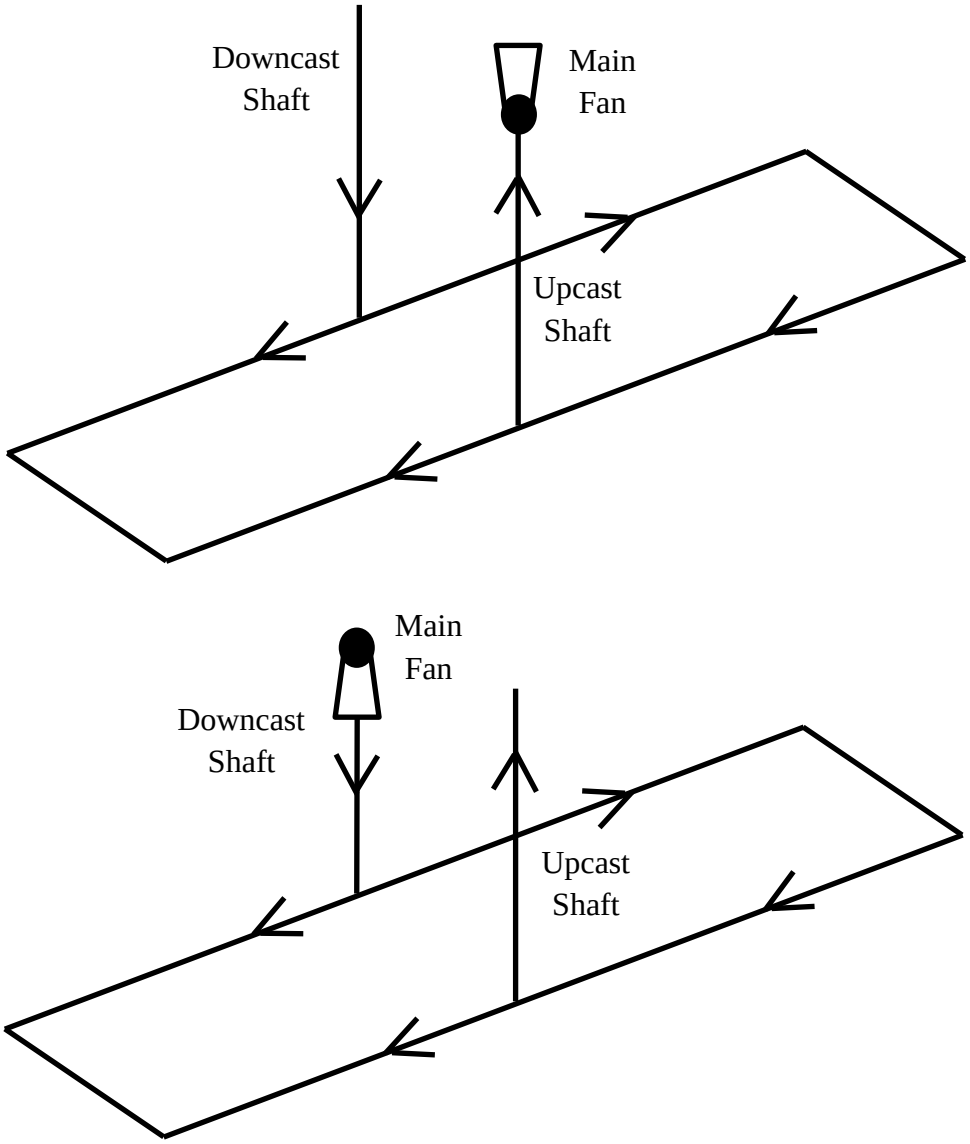

Figure 2.6: Ventilation systems, top: exhaust system; bottom: blower system (adapted from [34])

nodes along the branches (connected). A connected graph contains one or more spanning trees, which is defined as a set of branches that connect all the nodes without creating a closed loop. The branches that form part of this tree are known as the tree branches. The non-tree branches are known as chords [37] or links [38]. An independent mesh, or closed loop, is formed by adding just one link to the spanning tree, i.e. each independent loop will contain only one link. Thus the number of independent loops n_p is equal to the number of links, which can by calculated by Euler's polyhedron formula; $n_p = n - m + 1$, where n is the number of branches and m is the number of nodes.

To design and operate a mine ventilation system effectively, analysis of the network is required. This includes the determination of airflow rates and head loss in each airway or branch. The most common method used to solve these networks in the past, is the Hardy-Cross method. This method is an iterative process based on Kirchhoff's laws. Kirchhoff's first law says that "the algebraic sum of the flows at any pipe junction is zero"; and Kirchhoff's second law says that "the agebraic sum of the pressure drops around any closed loop (mesh) of the network is zero" [38, 39]. The Hardy-Cross method can thus be used to solve the network in two ways as described in [35]. The first method assumes initial values of flow rates that satisfy the first law; then they are corrected iteratively until the second laws are met. The second method assumes initial values of head at each node that satisfy the second law; then the flow rates are calculated and corrected iteratively until the first law is satisfied.

There has been other research succeeding this original theory, on solving flow networks. E.g. [40] shows an improved method which solves both Kirchhoff's laws simultaneously, using the Newton-Raphson method; [38] presents a computer program that uses an alternate technique to Hardy-Cross to solve the network. There have also been studies on solving the network by treating it as an optimization problem, e.g. [37] solves the problem using the Sequential Unconstraint Minimization Technique (SUMT); [41] solves the network using the GA technique; and [42] uses the Annealing method to solve the network. Most of these optimization problems formulate the constraints based on Kirchhoff's laws as follows:

Kirchhoff's current law is given by

$$\sum_{j=1}^{n} B_{ij} Q_j = 0, \text{ for } i = 1 \ldots m, \tag{2.5}$$

where j is the branch number, n is the total number of branches, Q_j is the flow rate of

branch j, i is the node number, m is the total number of nodes, B_{ij} is the element of an $m \times n$ incidence matrix $B = [B_{ij}]$ that describes the node-to-branch incidence:

$$B_{ij} = \begin{cases} 1, & \text{if flow in branch } j \text{ enters node } i; \\ -1, & \text{if flow in branch } j \text{ leaves node } i; \\ 1, & \text{if branch } j \text{ is not incident with node } i. \end{cases}$$

Kirchhoff's voltage law is adapted to paths, as opposed to meshes. A path in a network can be defined as a directed chain from the inlet node to the outlet node. In addition, airflows in all branches contained in the path must have the same direction. The total number of paths in a network is the same as the total number of independent meshes, n_p. Thus the KVL is given by

$$\sum_{j \in F} L_{pj} H_j - \sum_{j=1}^{n} L_{pj} h_j = 0, \text{ for } p = 1, \ldots, n_p, \tag{2.6}$$

where F is the set of branches containing a fan, H_j is the fan pressure in branch j, L_{pj} is an element of the path matrix $L = [L_{pj}]$, h_j is the pressure loss over the jth branch, p is the path number, and n_p is the total number of paths.

The path matrix L is an $n_p \times n$ matrix that describes the branch-to-path incidence and defined by

$$L_{pj} = \begin{cases} 1, & \text{if path } p \text{ contains branch } j; \\ 0, & \text{if path } p \text{ doesn't contain branch } j. \end{cases}$$

Unlike ohm's law, the relationship between pressure drop over a branch, or pipe, and the volumetric flow rate through it is not linear. It is derived from the Darcy-Weisbach equation [35] and is given by [37, 41]

$$h_j = R_j Q_j^2, \tag{2.7}$$

where h_j is the pressure drop over the branch j, Q_j is the flow rate through the branch j, and R_j is the resistance of branch j. The resistance of a pipe is derived in section 2.2, and given by eq. (2.4). This is a theoretical determination of the branch resistances. In practice,

however, the resistance of a branch would be found by using data for the for the flow rate and pressure differences obtained from meters inside the mine, and solving eq. (2.7) for R.

2.2.4 Ventilation costs

With the growing concerns of energy security and rising electricity prices, DSM activities have found its way into the mining industry. Research suggests that, depending on the type of mine, ventilation underground can consume between 20% and 40% of the total electricity used by the mine [8, 9]; and up to 60% of mining operating cost can be attributed to ventilation underground [10]. As such, there have been significant efforts to manage ventilation related costs.

Most studies aim to improve the overall efficiency of the ventilation system to achieve safe and economic solutions. Some studies make use of computer programmes, e.g. VUMA and VnetPC, in conjunction with survey data to model the changes in the structure of the mining network [43, 44]. Others include finding the optimal number, duty, and locations to install booster fans and regulators to reduce air leakage and improve flow distribution [45, 46].

The concept of ventilation on demand has stemmed from the ever increasing costs associated with mining at depth. Youngman [33] suggests that in the past, ventilation practices in South African mines have been wasteful; i.e. fans constantly running at the full production rate requirement, even when production is not at its peak. As such, profitability of mining at increased depths is seen as a concern for the future. Although in most mines, airflow control is part of the long term planning, i.e. at different stages of production, there is no control of the day-to-day or hour-by-hour needs. This is essentially what VOD addresses.

VOD aims to supply only the ventilation quantity required according to the production needs, which differ according to the area and time. In [7], a review is done at the beginning of every week to determine which levels will be inactive for the next week, such that the auxiliary fans in those levels can be switched off. A VOD project applied to a base metal mine in Canada, which spans over 2 km in depth, shows that the duty of a 112 kW fan can be controlled [5]. The projected savings are based on a period of 10 years, which is split into a development phase and a production phase. This is further split into two distinct airflow requirements in a day. Based on this, a 36.6% energy saving per year is predicted. Another

project, implemented by the same company in Canada, showed that by applying VOD to the auxiliary system and hence increasing available airflow quantity, other workings can be developed without increasing the total fresh air into the mine [47]. A similar study of a larger scale [48], totalling 7 860 kW, predicts a possible annual energy saving of 52.8%.

2.3 RESEARCH GAP

Existing studies on mine ventilation vary in objectives. The literature studied has shown that most studies are performed as part of an expansion plan, or with the aim of improving working conditions and efficiency of the entire system. These are usually not performed as a result of DSM initiatives, and don't consider LM or EE explicitly. Other studies, discussed in section 2.1.2, show the activities performed explicitly as a result of DSM, but none of these are applied to mine ventilation.

The only studies that consider DSM techniques in underground mine ventilation systems are the ones related to VOD. These studies perform EE measures by application of VSDs, but there is no consideration for shifting load from peak times and the TOU tariff. Another drawback to these studies is that only auxiliary fans are focused on, as opposed to the main fan. The main reason for this is that changing the speed of the main fan will affect the entire network, and is more complicated to control than the auxiliary fans.

Thus little evidence is found of application of EE and LM simultaneously, in particular, to mining ventilation networks. To this end, this research focuses on controlling the main fan in a ventilation network to obtain both, energy and cost savings.

2.4 CHAPTER SUMMARY

This chapter presented the literature reviewed. The main focus was on DSM techniques and underground mining ventilation networks. Various studies were found with different objectives, relating to these topics individually; but little research exists which combine these two areas together. This is what lead to the research gap, and the objectives of this study.

CHAPTER 3

PROBLEM FORMULATION

This chapter presents the formulation of the optimization models that are used to find the maximum possible cost saving in underground mine ventilation networks. Part of this model formulation includes the derivation of the operating point of a fan, which is also discussed. This involves incorporating the fan laws and the network's system curve to get a realistic figure of the savings.

The problem is divided two parts, i.e. EE and LM. For the EE case, energy consumption is minimized by determining an optimal speed profile for the main fan according to VOD. For the LM case, the mine schedule is optimized considering the TOU tariff, such that further energy cost reduction can be achieved for the mine. The ventilation network is first mathematically modelled by extending the work shown in [37, 41]. Thereafter, the fan speed optimization problem is solved to determine the optimal fan speed profile that matches the VOD requirements and minimizes energy consumption. Then, the optimal starting time of a mining schedule is found by solving another optimization problem formulated, to find the total possible cost saving.

3.1 FAN LAWS AND PERFORMANCE CURVES

A particular fan can be characterized by its fan curve, i.e. how much pressure the fan needs to develop to supply a particular flow rate. A simple example of fan curves is shown in fig. 3.1. It can be seen that a fan running at a particular speed has its corresponding fan curve, therefore changing the speed will result in a new curve. It can also be seen that as the speed reduces, a lower head, or pressure, is required to achieve the same flow rate. This

means less power is needed to supply the fan, since the air power is given as the product of the pressure and the flow rate. Thus less power is consumed at lower running speeds [27]. However, the question arises as to how to characterize the relationship between flow rate and power. This is solved by the Fan Laws, also known as the Affinity Laws.

The Fan Laws are a set of governing equations that define the relationship between the speed of the fan *(N)*, the pressure developed by the fan *(H)*, and the input power to the fan *(P)*. These laws are given as [49]

$$\frac{Q_1}{Q_2} = \frac{N_1}{N_2}, \tag{3.1}$$

$$\frac{H_1}{H_2} = (\frac{N_1}{N_2})^2, \tag{3.2}$$

$$\frac{P_1}{P_2} = (\frac{N_1}{N_2})^3. \tag{3.3}$$

In these equations, the variables with subscript 1 are those at the original condition, and the ones with subscript 2 are the resulting variable due to the change in speed. E.g. Using the first formula, the new flow rate (Q_2) can be found, due to the change in speed, if the initial flow rate (Q_1) is known. The same idea can be applied to the formulas regarding the pressure and power, respectively.

3.2 SYSTEM CURVES

The system curve represents the combination of all the aerodynamic resistances in the system, by simplifying the entire network into a single airway with an equivalent resistance. Thus, it defines the relationship between the flow rates through an airway that will be achieved, given the supply pressures over that airway [34].

For instance, in fig. 4.1, the system curve can be found by finding the equivalent resistance seen from the fan's point of view. Ideally, the system curve is characterized by a second order function in the same form as eq. (2.7). Practically, however, the following equation is taken as the general form to cater for offsets and disturbances

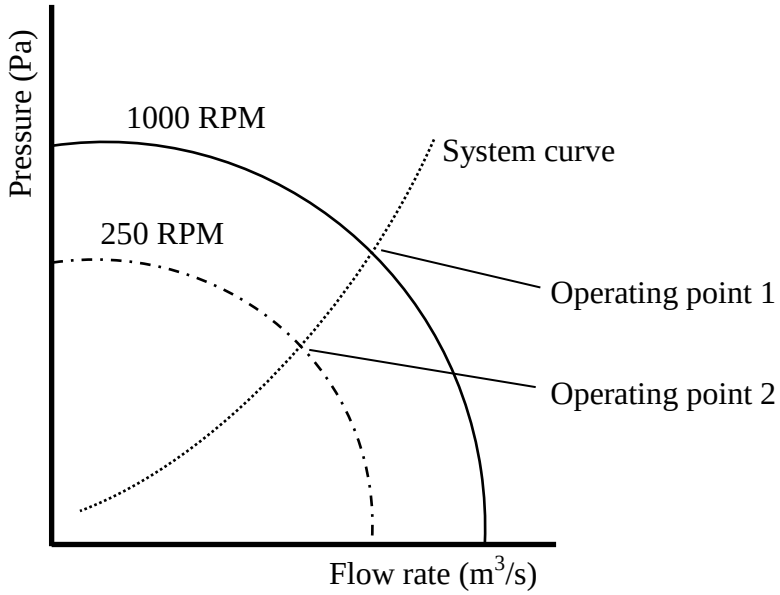

Figure 3.1: Operating points at different fan speeds

$$H = b_2 Q^2 + b_1 Q + b_0. \tag{3.4}$$

In order to find the total equivalent resistance, some equivalent resistance simplifications are necessary. Usually, a network is termed simple if it only contains airways in parallel and series, which can be reduced to one equivalent airway. For airways in series, the following simplification can be made [50]

$$R_{eq} = R_1 + R_2. \tag{3.5}$$

For parallel airways,

$$\frac{1}{\sqrt{R_{eq}}} = \frac{1}{\sqrt{R_1}} + \frac{1}{\sqrt{R_2}}. \tag{3.6}$$

A simple network, however, is unlikely to find in practice. Thus networks that cannot be simplified by just using parallel and series combination are termed complex networks. The network shown in fig. 4.1 is an example of complex network. As can be seen, it is not possible

to simplify the network to a single airway with just series and parallel combinations. Thus two methods are presented to find the equivalent resistance of complex networks.

The first method involves adding a test fan, after which, the network is solved iteratively to get an approximate solution for the flow rates of all the branches, while adhering to Kirchoff's laws as shown in eqs. 3.20 and 3.21. The equivalent resistance is then given by $R_{eq} = \frac{H_{test}}{Q_{test}^2}$ [34], where H_{test} is the pressure of the test fan and Q_{test} is the flow rate of the branch that contains the test fan. This procedure is similar to finding the Thevenin equivalent in circuit theory [39]. Although this procedure is quite quick to find the equivalent resistance, the fact that an iterative process is used means the solution is an approximation.

Thus, another method is devised to find the correct value of the equivalent resistance. This method is a bit more tedious, but will lead to a more accurate result. It involves simplifying the network by using a delta-wye transform, along with the parallel and series combinations. For a delta to wye conversion, with reference to fig. 3.2, the following equations are derived from first principles

$$\begin{aligned} 2R_1 = &\frac{R_c(R_a+R_b)}{R_a+R_b+R_c+2\sqrt{R_c(R_a+R_b)}} \\ &+\frac{R_b(R_a+R_c)}{R_a+R_b+R_c+2\sqrt{R_b(R_a+R_c)}} \\ &-\frac{R_a(R_b+R_c)}{R_a+R_b+R_c+2\sqrt{R_a(R_b+R_c)}}, \end{aligned} \tag{3.7}$$

$$\begin{aligned} 2R_2 = &\frac{R_a(R_b+R_c)}{R_a+R_b+R_c+2\sqrt{R_a(R_b+R_c)}} \\ &+\frac{R_c(R_a+R_b)}{R_a+R_b+R_c+2\sqrt{R_c(R_a+R_b)}} \\ &-\frac{R_b(R_a+R_c)}{R_a+R_b+R_c+2\sqrt{R_b(R_a+R_c)}}, \end{aligned} \tag{3.8}$$

$$\begin{aligned} 2R_3 = &\frac{R_a(R_b+R_c)}{R_a+R_b+R_c+2\sqrt{R_a(R_b+R_c)}} \\ &+\frac{R_b(R_a+R_c)}{R_a+R_b+R_c+2\sqrt{R_b(R_a+R_c)}} \\ &-\frac{R_c(R_a+R_b)}{R_a+R_b+R_c+2\sqrt{R_c(R_a+R_b)}}. \end{aligned} \tag{3.9}$$

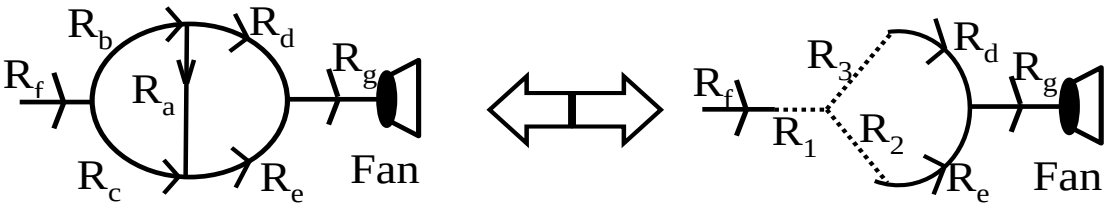

Figure 3.2: Delta to Wye Conversion

Thus, the equivalent resistance as seen from the fan's point of view in fig 3.2 is calculated by

$$R_{eq} = R_f + R_1 + ((R_3 + R_d)||(R_2 + R_e)) + R_g. \tag{3.10}$$

Hence, the coefficient b_2 in eq. (3.4) is found by the above calculations to be $b_2 = R_{eq}$. The other coefficients in the equation are considered to be 0 in this study, because an ideal case is assumed.

In practice, the equivalent resistance is found by first finding the the resistance of each branch. This is done by obtaining data for the flow rate and pressure differences from meters inside the mine, then the square law $H = RQ^2$ is used to find R. The iterative method described above would then be used to determine the equivalent resistance. For this research, due to the lack of data, it is assumed that the resistance for each branch is known already and the system curve is derived from these values. Both methods described above are used in chapter 4 to find the equivalent resistance, and it is shown that both are acceptable.

3.3 FAN OPERATING POINT

When analyzing flow rate, pressure, and power changes of a fan with respect to speed changes; often the fan, or affinity laws, are used. However, this is only valid when the fan is being analyzed by itself. When considering the fan as part of a network, using only the fan laws will result in incorrect analysis, i.e. there is no guarantee that the fan will operate at the calculated flow rate and/or pressure. More importantly, a reduction in fan speed will often result in an overestimate of power savings [51]. When formed part of a network, the fan will operate at a steady state condition, which is known as the operating point of the fan. The operating point of a fan is the intersection point between the fan curve and the system

curve of the network, in which the fan is situated. A simple example of this is shown in fig. 3.1. It can be seen that if the fan is running at 1000 RPM, it will operate at point 1, and if it is running at 250 RPM, it will operate at point 2. This shows that every time the speed changes, there will be a new operating point. Thus, it is imperative that the affinity laws are used in conjunction with the system curve, such that the correct operating point is found.

In section 3.4, three equations are used as part of the objective and constraints, i.e. $P_k(N_k(t))$, $Q_k(N_k(t))$, and $H_k(N_k(t))$. These equations express the power, the flow rate, and the pressure as a function of the fan speed, respectively. The fan operating point $[H_k(N_k(t)), Q_k(N_k(t))]$ is time varying for VSDs and determines the power consumption of the fan $P_k(N_k(t))$. Therefore, the procedure to derive these equations is shown in this section.

For the ease of notation, the subscript k in the functions $P_k(N_k(t))$, $Q_k(N_k(t))$ and $H_k(N_k(t))$ is omitted in the remaining of this section. For each fan k, the same procedure as given here applies. This research is based on the analytical approach by making use of the fan manufacturer's datasheet.

To form the flow-speed function $Q(N(t))$, the fan curve of the highest speed is required. This curve can be described by a second order polynomial given by the generic form

$$H_{full} = a_2 Q_{full}^2 + a_1 Q_{full} + a_0, \tag{3.11}$$

where H_{full} is the pressure developed by the fan at full speed, Q_{full} is the flow rate delivered by the fan at full speed; a_2, a_1, and a_0 are constant parameters derived from the full speed fan curve.

By making use of the fan laws, and replacing eqs. (3.1) and (3.2) into eq. (3.11), the following equation is obtained

$$H = a_2 Q^2 + a_1 Q \frac{N}{N_{full}} + a_0 \left(\frac{N}{N_{full}} \right)^2 \tag{3.12}$$

where N_{full} is the rated full-speed, and H is the pressure developed by the fan at any speed, N.

By equating eq. (3.12) to the system curve equation (3.4) and solving for Q, a function is obtained for the flow rate only in terms of the normalized speed ($\frac{N}{N_{full}}$) [52]. By curve fitting, this function can be approximated to a linear function given by

$$Q(N(t)) = c_1 \frac{N(t)}{N_{full}} + c_0, \tag{3.13}$$

where c_1, and c_0 are constant parameters.

Thus, eq. (3.13) can be used to find the flow rate at the operating point corresponding to any given fan speed $N(t)$.

The pressure-speed function is obtained in a similar method, i.e. the same procedure is followed until eq. (3.12) is reached. Thereafter, eq. (3.12) and eq. (3.4) are each expressed in terms of the flow rate Q. These are then equated to each other, and then the resulting equation is solved for H. This will result in a function for the pressure developed by the fan expressed only in terms of the normalized speed. Again, by curve fitting, this function can be approximated to a second order polynomial given by the generic form

$$H(N(t)) = d_2 \left(\frac{N(t)}{N_{full}} \right)^2 + d_1 \frac{N(t)}{N_{full}} + d_0. \tag{3.14}$$

Lastly, with the fan operating point find by eqs. (3.13) and (3.14), the power of the fan at the operating point is obtained by following a similar process to the flow-speed formulation. First, the power curve for the highest speed is expressed as a 3rd order polynomial; into which, eqs. (3.1) and (3.3) are replaced to yield the following equation

$$P = e_3 Q^3 + e_2 Q^2 \frac{N}{N_{full}} + e_1 Q \left(\frac{N}{N_{full}} \right)^2 + e_0 \left(\frac{N}{N_{full}} \right)^3. \tag{3.15}$$

Thereafter, by replacing eq. (3.13) into eq. (3.15), a function is obtained for the power only in terms of the normalized speed [32]. By curve fitting, this function can be approximated to a 3rd order polynomial given by the generic form

$$P(N(t)) = f_3 \left(\frac{N(t)}{N_{full}} \right)^3 + f_2 \left(\frac{N(t)}{N_{full}} \right)^2 + f_1 \frac{N(t)}{N_{full}} + f_0, \tag{3.16}$$

After eq. (3.16) is obtained, the power of the fan operating at different speeds can be calculated accurately with the fan's operating point accounted for.

3.4 ENERGY EFFICIENCY

In this section the formulation of a generic optimization model is given, that finds the optimal fan speeds that result in minimum energy cost, while adhering to the VOD requirements.

The objective is to minimize the following discrete cost function

$$J = \sum_{k=1}^{K} \sum_{t=1}^{T} P_k(N_k(t))C(t)\Delta t, \tag{3.17}$$

where K is the total number of fans, T is the total number time steps, $C(t)$ is the time of use tariff at time step t, and Δt is the length of time steps in hours.

$P_k(N)$ is a 3rd order polynomial that describes the power consumption of the fan k as a function of its speed $N_k(t)$, which is a function of time. It is detailed in section 3.3 and given in eq. (3.16).

Since the optimization variable is chosen to be the fans' speeds, the flow rates of the branches that contain a fan are defined by flow rates of that fan. This forms the first system constraint, given by

$$Q_j(t) = Q_k^j(N_k(t)), \text{for } j \in F, \tag{3.18}$$

where $Q_j(t)$ and $Q_k^j(N_f(t))$ are the flow rate of branch j and the flow rate of fan k that lie in branch j at time t, respectively.

$Q_k^j(N_k(t))$ is a linear equation that describes the flow rate of a fan k, as a function of its speed $N_k(t)$. It is given by eq. (3.13) in section 3.3.

The second constraint is based on the ventilation load of the mine. This is where the concept of VOD is used, i.e. the demand for airflow rate at each branch, at each time step forms the load to the system. This can be written as

$$Q_j^{min}(t) \leqslant Q_j(t) \leqslant Q_j^{max}(t), \tag{3.19}$$

where $Q_j^{min}(t)$ and $Q_j^{max}(t)$ are the minimum and maximum allowable airflow in branch j at time t. For the case where the demand is a fixed amount, $Q_j^{min}(t) = Q_j^{max}(t)$.

The rest of the constraints are formed based on the principles of conservation of mass and energy. The principle of conservation of mass is stated in eq. (2.5), but is shown here again including the time variable.

$$\sum_{j=1}^{n} B_{ij} Q_j(t) = 0 \text{ for } i = 1, \ldots, m. \tag{3.20}$$

The principles of conservation of energy is expanded from eq. (2.6) to give

$$\sum_{j \in F} L_{pj} H_j(t) - \sum_{j=1}^{n} L_{pj} r_j Q_j^2(t) = 0, \text{ for } p = 1...n_p, \tag{3.21}$$

where $H_j(t)$ is the fan pressure in branch j at time t. For a specific fan k, this is a second order polynomial that describes the pressure across the fan as a function of its speed $N_k(t)$ at time t and denoted as $H_k(N_k(t))$, which is derived from the fan laws, and is presented in eq. (3.14) in section 3.3.

Thus an optimization model can be completely described by the objective function, given by eq. (3.17), and the constraints, given by eqs. (3.18) - (3.21).

3.5 LOAD MANAGEMENT

To further reduce energy costs, the potential of peak shaving and cost minimization by implementation of load shifting is investigated. It is assumed that a mining schedule consists of N processes that follow each other. Each of these processes have a particular flow rate requirement, which can be associated with a power value. Thus the idea is to find the optimal starting point of the schedule in view of the TOU tariff, that will result in minimum cost.

To do so, the following cost function is minimized

$$J = \sum_{i=t_s}^{\lambda_1 - 1} P_1 C(i) + \sum_{i=\lambda_1}^{\lambda_2 - 1} P_2 C(i) + \cdots + \sum_{i=\lambda_{N-1}}^{\lambda_N - 1} P_N C(i), \tag{3.22}$$

where t_s is the starting time of the schedule, and the decision variable; $P_1, \ldots, P_N$ are the power consumptions (kW) associated with tasks 1 to N; $C(i)$ is the electricity cost (R/kWh) at time instant i, according to the TOU tariff; and

$$\lambda_y = t_s + \sum_{z=1}^{y} t_{p(z)}, \text{for } y = 1 \ldots N. \tag{3.23}$$

where $t_{p(1)}, \ldots, t_{p(N)}$ are the durations (hours) of the tasks 1 to N. It is assumed in this study that $t_{p(N)}$ can only take integer values.

3.6 VALIDATION OF MODEL

The nature of the problem can be described as multi-variable, non-linear, constrained optimization. The non-linearity appears in the objective, as well as the constraints. The optimization variables are the fan speeds and the flow rates in all the branches, i.e. more than 1, which makes it multi-variable. The solution space is also continuous. Thus in view of the foregoing and literature reviewed, it was decided that the *fmincon* function in *Matlab* would be used to solve this problem. Various algorithms were also tested, including the *interior point*, *trust-region-reflective*, *sequential-quadratic-programming (SQP)*, and *active-set*. In order to validate the developed model and the algorithms, a simple network (whose solution was theoretically calculated) was simulated for one time instant; the result of this was then compared to the worked out solution. It was found that the best results were obtained when the *SQP* algorithm was used. The test performed is described below.

The simple network shown in fig. 3.3 was used for the validation. The data for the fan is also known (given in appendix A.1). It can be seen that there are 7 branches, 5 nodes, and therefore 3 independent paths. To make the theoretical calculations easier, it is assumed that all branches in the network has a resistance of 0.001 Ns^2/m^8.

Assuming all branches have a lower bound on the flow rate of 50 m^3/s, the flow rate in each branch can be theoretically calculated that will lead to the minimum power consumption by

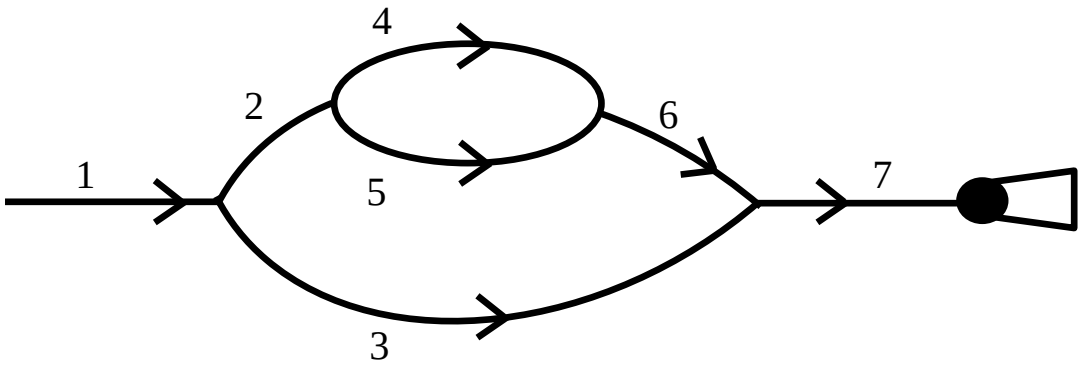

Figure 3.3: Network for validation test

the fan. To solve the network, the following procedure is followed:

1. It is first assumed that branches 4 and 5 will have the same flow rate (because they are in parallel).

2. Choosing the flow rate of branches 4 and 5 to be equal to the lower bound of 50 m^3/s leads to the flow rate in branches 2 and 6 to be 100 m^3/s each, from KCL.

3. It is also known that the flow rate in branches 1 and 7 will be the same, from KCL.

4. Thus, three equations can be formed and solved simultaneously. The first two are formed from KVL, and the last one from the operating point of the fan derived as shown in section 3.3. These are given by

$$R_1Q_1^2 + R_2Q_2^2 + R_5Q_5^2 + R_6Q_6^2 + R_7Q_7^2 - H_f(Q_7) = 0,$$

$$R_1Q_1^2 + R_3Q_3^2 + R_7Q_7^2 - H_f(Q_7) = 0,$$

$$H_f(Q_7) = 511.45(\tfrac{Q_7}{750})^2.$$

The unknown variables in the equations above are Q_1, Q_3, and H_f. All the other variables are known. The solution is shown in table 3.1. It is noted that for this case, this solution is indeed optimal, i.e. no other set of flow rate values will result in a lower fan power consumption, while adhering to the constraints. Thus, the algorithm was run in *Matlab* and the same results were obtained, showing the validity of the model. To further validate the model, the network was also modelled using the *solver* function in *Microsoft Excel*, which also gave the

same results.

Table 3.1: Theoretical solution for example shown in fig. 3.3

Branch no.	Lower bound (m^3/s)	Calculated solution (m^3/s)	Model optimal solution (m^3/s)
1	50	250	250
2	50	100	100
3	50	150	150
4	50	50	50
5	50	50	50
6	50	100	100
7	50	250	250

Another test was performed as part of the validation process. All conditions were kept the same, except the bounds on the flow rate in branches 4 was chosen to be 30 $m^3/s \leq Q_4 \leq$ 40 m^3/s. Thus the upper bound of branch 4 was chosen to be less than the lower bound of branch 5, i.e. branches 4 and 5 could not have the same flow rate unless the resistance of the branches were changed by use of regulators. Therefore no solution exits for this case because the branches, being in parallel and having the same resistance, must have the same flow rate. This case was simulated, and the model was not able to converge to a solution, as expected. In view of the foregoing, it was decided that the model can be adapted to the complicated network (see fig. 4.1) used for this study, and the SQP algorithm should be used under the $fmincon$ function to simulate the network.

3.7 CHAPTER SUMMARY

Two optimization models were presented in this chapter, i.e., the EE and LM. To develop these models, the use of network theory and fan laws are necessary, which are also shown. The model was validated using a simple network and *Microsoft Excel*, and was found to be accurate.

The procedure followed, to determine the maximum savings for a particular ventilation network, is summarized in fig. 3.4.

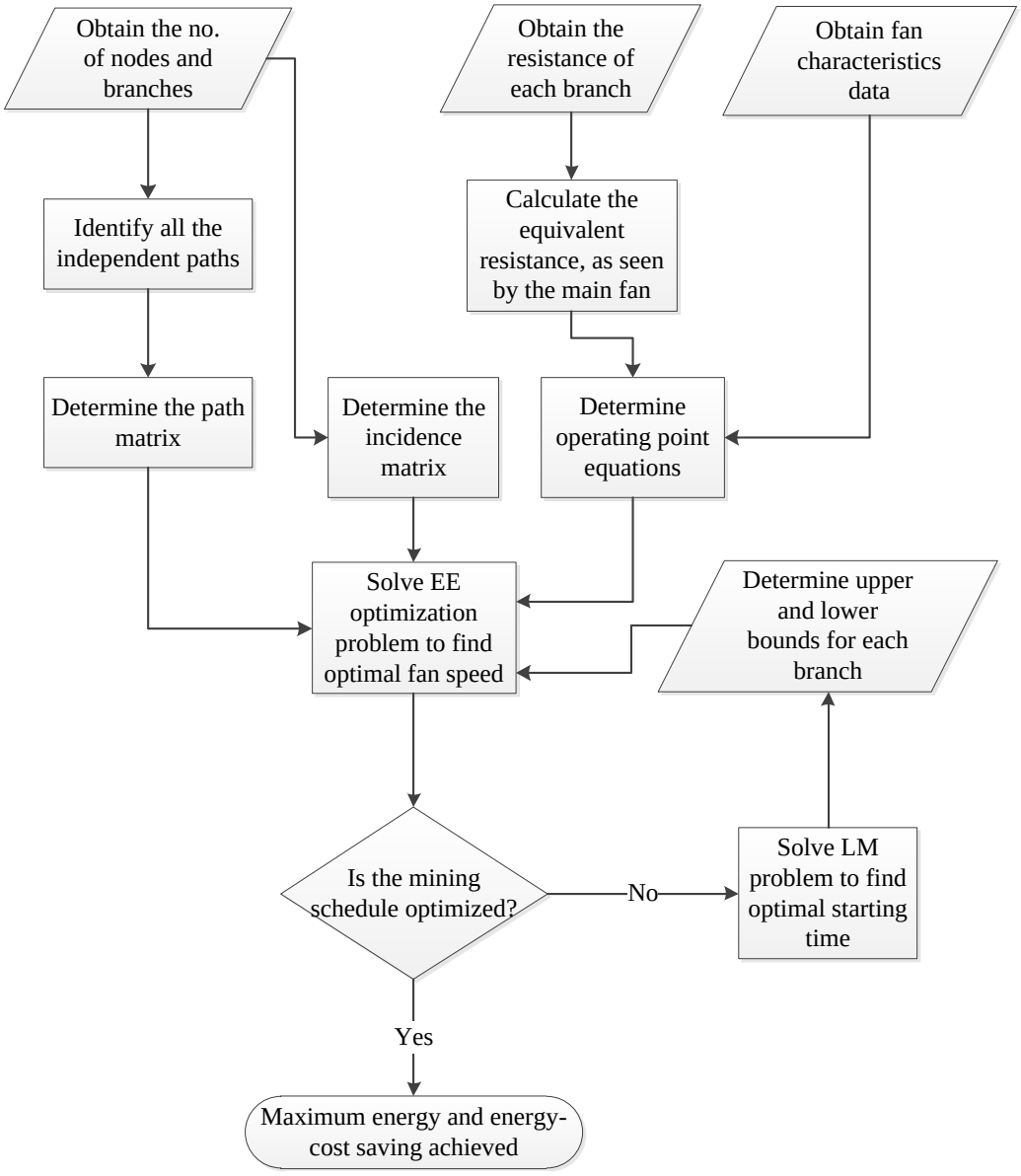

Figure 3.4: Flow chart showing test procedure

CHAPTER 4

CASE STUDY

For demonstration purposes, a case study is presented. All the generic approaches presented in the previous sections are applied to the network shown in fig. 4.1. The operating point of the fan is determined, relative to the network. Then, the two optimization problems, i.e. EE and LM, are analyzed. They are first analyzed individually, after which, they are combined to investigate the maximum possible cost savings. Various conditions are also simulated to compare the effects on the savings of different scenarios.

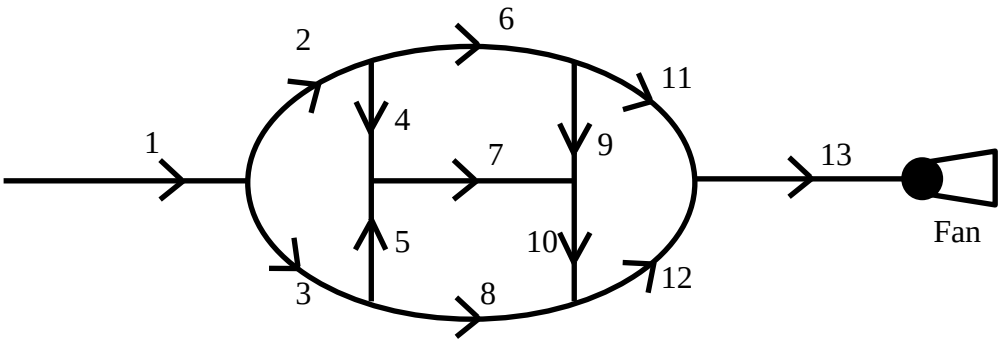

Figure 4.1: An example of a ventilation network (adapted from [37]).

4.1 PROBLEM DESCRIPTION

It is assumed that any branch where mining activity is taking place, follows a fixed cycle. This cycle contains a set of tasks, where each task has an associated minimum flow rate requirement and duration. An arbitrary cycle is shown in table 4.1, however the flow rate values shown are obtained from literature. It must also be noted that the processes shown must follow each other, i.e. they are shown in chronological order.

Table 4.1: Mining cycle and its requirements(adapted from [5])

Process	Duration	Min. flow rate required (m^3/s)
Drilling	8 hours	15.2
Explosive charge-up	3 hours	10.3
Blasting	6 hours	none
Cleaning & Mucking	7 hours	25.5

The price of energy, according to time of use, is usually dependant on the time of day, weekday vs. weekend, and season of year. In South Africa, a day is divided into a maximum of three different rates; namely off-peak, standard, and peak. A year is divided into 2 seasons, namely high demand (which runs from June to August), and low demand (which runs from September to May).

Tables 4.2, 4.3, and 4.4 show the tariff structures that apply during high demand season for a weekday, Saturday and Sunday, respectively. During low demand season the time of use period remains the same as the high demand season, however the rates are cheaper, which is shown in table 4.5.

Table 4.2: Megaflex weekday TOU tariff during high demand season

Time of day	Tariff (R/kWh)
00:00 - 06:00 (off-peak)	0.348
06:00 - 07:00 (standard)	0.641
07:00 - 10:00 (peak)	2.116
10:00 - 18:00 (standard)	0.641
18:00 - 20:00 (peak)	2.116
20:00 - 22:00 (standard)	0.641
22:00 - 24:00 (off-peak)	0.348

Table 4.3: Megaflex Saturday TOU tariff during high demand season

Time of day	Tariff (R/kWh)
00:00 - 07:00 (off-peak)	0.348
07:00 - 12:00 (standard)	0.641
12:00 - 18:00 (off-peak)	0.348
18:00 - 20:00 (standard)	0.641
20:00 - 24:00 (off-peak)	0.348

Table 4.4: Megaflex Sunday TOU tariff during high demand season

Time of day	Tariff (R/kWh)
00:00 - 24:00 (off-peak)	0.348

Table 4.5: Megaflex tariff during low demand season

Period	Tariff (R/kWh)
Peak	0.69
Standard	0.48
Off-peak	0.30

4.2 SYSTEM CURVE

The system curve is found by following the steps shown in section 3.2. As stated earlier, for this research it is assumed that the resistance of each branch is known. The network and the resistance values shown in [37] are used for this study (see table 4.6). The equivalent resistance is thus derived using these resistance values.

Table 4.6: Resistance values for the example network (adapted from[37])

Branch no.	Resistance (Ns^2/m^8)
1	0.0225
2	0.1104
3	0.3
4	0.168
5	3.6
6	0.15
7	0.072
8	1.35
9	0.225
10	0.0551
11	4.5
12	0.0385
13	0.0585

One way of obtaining the equivalent resistance is by using a test fan as a source, and solving for all the flow rates in the branches iteratively as shown in [34]. Thus a test fan, operating at 10 Pa, was added in branch 13 and the network was solved using the solver add-in in Microsoft Excel.

The solution is shown in table 4.7. The flow rates were selected as the independent variables to optimize.

The KCL equations were chosen to be the constraints. As shown in table 4.8, there are 9 nodes, which all satisfy KCL, i.e. the sum of flow rates going into each node is equal to the

Table 4.7: Solution to find R_{eq}

Branch No.	Resistance	Flowrate	Pressure Loss
1	0.0225	6.83	1.05
2	0.1104	4.59	2.33
3	0.3	2.24	1.51
4	0.168	2.20	0.82
5	3.6	0.67	1.63
6	0.15	2.39	0.86
7	0.072	2.88	0.60
8	0.1.35	1.57	3.32
9	0.0.225	1.57	0.55
10	0.0551	4.44	1.09
11	4.5	0.82	3.03
12	0.0385	6.01	1.39
13	0.0585	6.83	2.73

sum of flow rates leaving that node.

The sum of the squares of the KVL equations was chosen as the objective to minimize. Table 4.9 shows that the sum of pressure drops over each path is very close to zero, which results in the objective value to be 7.18×10^{-11}.

Thus the equivalent resistance of the network can be calculated by $R_{eq} = \frac{H_{test}}{Q_{test}^2}$, where $H_{test} = 10$ is the pressure of the test fan and Q_test=6.83 is the flow rate of the branch that contains the test fan. This results in the equivalent resistance of the entire network to be R_{eq}=0.214 Ns^2/m^8.

The other method to find the equivalent resistance is by use of delta-wye transformations, along with series and parallel simplifications of the network. With reference to fig. 3.2 and eqs. (3.7), (3.8), and (3.9), the logical steps taken to find the equivalent resistance is shown in fig. 4.2. The resulting resistances after each step are indicated adjacent to the branches. It can be seen that after the entire network is simplified to result in one airway, the equivalent resistance is R_{eq}=0.2122 Ns^2/m^8. It is noted that this value is very close to the value obtained

Table 4.8: KCL equations used as constraints in finding R_{eq}

Node	Sum	Description
1	0	$Q_1 - Q_2 - Q_3$
2	0	$Q_2 - Q_4 - Q_6$
3	0	$Q_4 + Q_5 - Q_7$
4	0	$Q_3 - Q_5 - Q_8$
5	0	$Q_6 - Q_9 - Q_11$
6	0	$Q_7 + Q_9 - Q_10$
7	0	$Q_8 + Q_10 - Q_12$
8	0	$Q_11 + Q_12 - Q_13$
9	0	$Q_13 - Q_1$

Table 4.9: KVL equations used as part of the objective in finding R_{eq}

Path	Sum($\times 10^{-6}$)	Description
1	-6.63	$R_1Q_1^2 + R_2Q_2^2 + R_6Q_6^2 + R_{11}Q_{11}^2 + R_{13}Q_{13}^2 - H_{fan}$
2	-1.23	$R_1Q_1^2+R_2Q_2^2+R_4Q_4^2+R_7Q_7^2+R_{10}Q_{10}^2+R_{12}Q_{12}^2+R_{13}Q_{13}-H_{fan}$
3	0.66	$R_1Q_1^2+R_2Q_2^2+R_6Q_6^2+R_9Q_9^2+R_{10}Q_{10}+R_{12}Q_{12}^2+R_{13}Q_{13}-H_{fan}$
4	-4.18	$R_1Q_1^2 + R_3Q_3^2 + R_8Q_8^2 + R_{12}Q_{12}^2 + R_{13}Q_{13} - H_{fan}$
5	-2.90	$R_1Q_1^2+R_3Q_3^2+R_5Q_5^2R_7Q_7^2+R_{10}Q_{10}^2+R_{12}Q_{12}^2+R_{13}Q_{13}-H_{fan}$

by the iterative method to calculate R_{eq}, thus showing that either method is acceptable to find the equivalent resistance. However, since the iterative method finds the result based on approximations, the delta-wye method is assumed to be more accurate, and hence the value obtained from this method is used.

Thus assuming an ideal case, the system curve is given by

$$H = 0.2122Q^2. \tag{4.1}$$

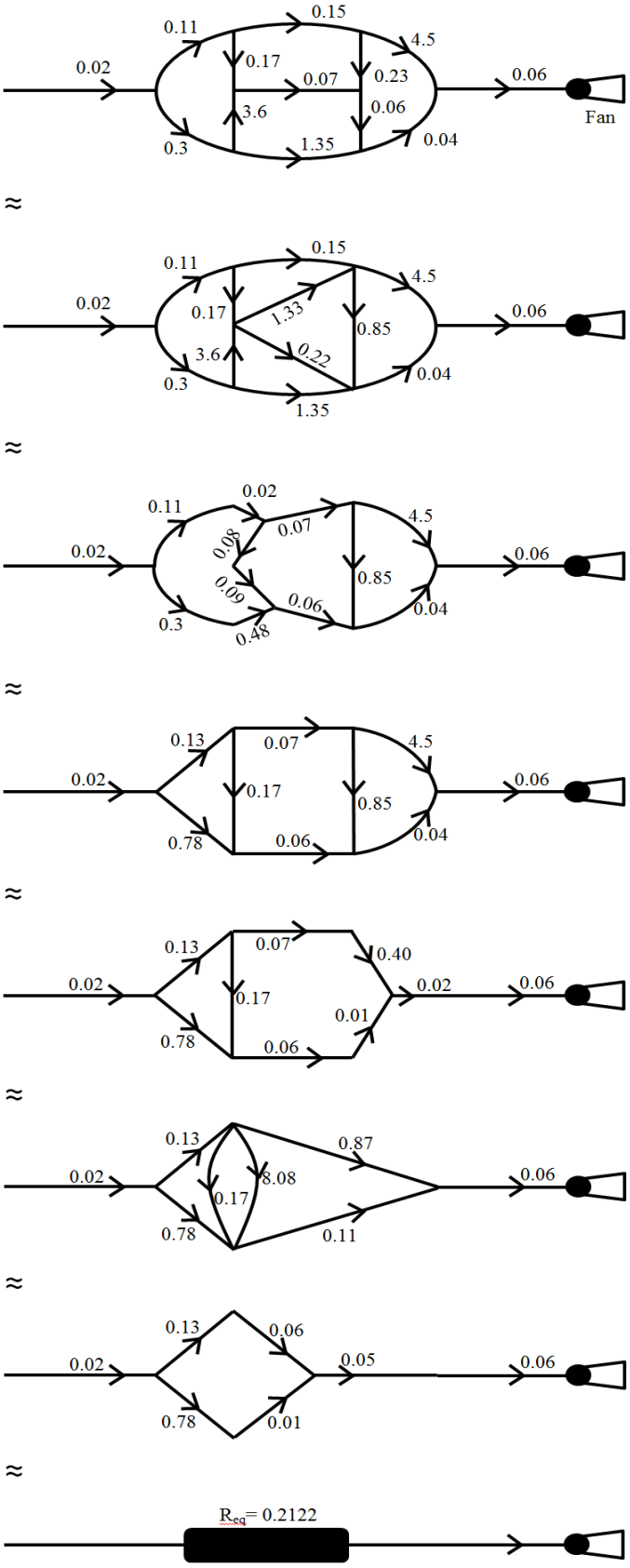

Figure 4.2: Steps to find R_{eq}

4.3 OPERATING POINT

In order to find the optimal speeds to minimize energy cost; the power, pressure, and flowrate have to be given as a function of the fan speed. This is done by making use of a fan's datasheet. The fan curve is plotted for a fan running at 750 RPM (see fig. 4.3).

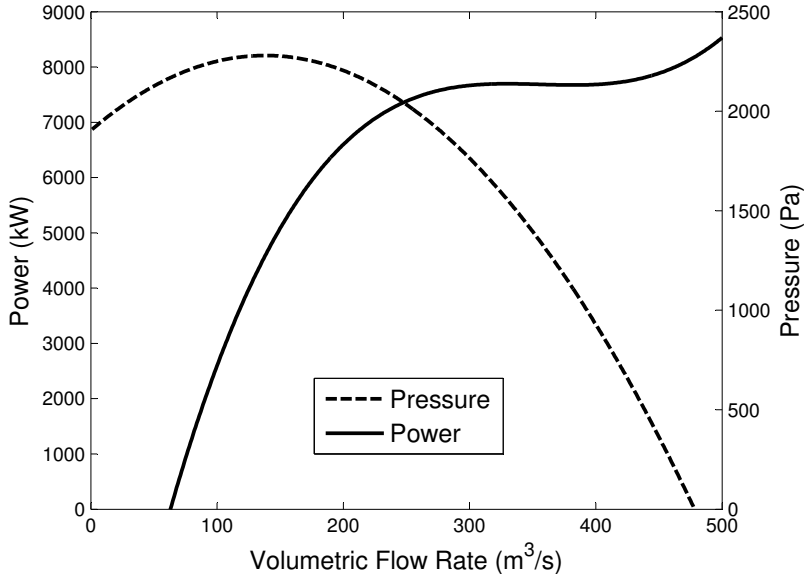

Figure 4.3: Fan power and performance curve

The data for this curve is obtained from an operating mine in South Africa. Thereafter, the procedure shown in section 3.3 is followed to obtain the necessary functions.

The power-speed, pressure-speed, and flow-speed functions are given by eqs. (4.2), (4.3), (4.4) respectively. The actual derivation of these functions and the data used for the fan is shown in Appendix A.1.

$$P(N) = 1796(\frac{N}{750})^3, \tag{4.2}$$

$$H(N) = 7973(\frac{N}{750})^2, \tag{4.3}$$

$$Q(N) = 193.8(\frac{N}{750}). \tag{4.4}$$

4.4 ENERGY EFFICIENCY

To optimize the fan speeds according to the VOD requirements, eq. (3.17) is used as the objective function. There is only one fan in the network, thus $k = 1$; the total no. of time steps is $T = 24$ hours; the sample size is $\Delta t = 1$ hour; the reference speed is 750 RPM; and using the power-speed function derived in section 4.3, the objective function applicable to this study can be written as

$$J = \sum_{t=1}^{24} 1796 \left(\frac{N_t}{750} \right)^3 C(t). \tag{4.5}$$

The first constraint, given by eq. (3.18), says that the flow rate of the branch that contains a fan is equal to the flow rate given by the fan. There is only one fan (in branch no. 13); thus by using this fact and the flow-speed equation derived in section 4.3, the constraint that is applicable to this study can be written as

$$Q_{13}(t) = 193.8(\frac{N_t}{750}). \tag{4.6}$$

In the selected network there are 13 branches, thus $n = 13$; and 9 nodes, thus $m = 9$. The KCL constraint given by eq. (3.20), can therefore be written as

$$\sum_{j=1}^{13} B_{ij} Q_j(t) = 0, \text{ for } i = 1 \ldots 9, \tag{4.7}$$

where the the incidence matrix, B_{ij}, is given by

$$B = \begin{bmatrix} 1 & -1 & -1 & 0 & 0 & 0 & 0 & 0 & 0 & 0 & 0 & 0 & 0 \\ 0 & 1 & 0 & -1 & 0 & -1 & 0 & 0 & 0 & 0 & 0 & 0 & 0 \\ 0 & 0 & 0 & 1 & 1 & 0 & -1 & 0 & 0 & 0 & 0 & 0 & 0 \\ 0 & 0 & 1 & 0 & -1 & 0 & 0 & -1 & 0 & 0 & 0 & 0 & 0 \\ 0 & 0 & 0 & 0 & 0 & 1 & 0 & 0 & -1 & 0 & -1 & 0 & 0 \\ 0 & 0 & 0 & 0 & 0 & 0 & 1 & 0 & 1 & -1 & 0 & 0 & 0 \\ 0 & 0 & 0 & 0 & 0 & 0 & 0 & 1 & 0 & 1 & 0 & -1 & 0 \\ 0 & 0 & 0 & 0 & 0 & 0 & 0 & 0 & 0 & 0 & 1 & 1 & -1 \\ -1 & 0 & 0 & 0 & 0 & 0 & 0 & 0 & 0 & 0 & 0 & 0 & 1 \end{bmatrix}.$$

The number of independent paths, $n_p = n-m+1 = 5$; and there is only one branch containing a fan (no. 13). By using these facts and the pressure-speed equation derived in section 4.3, the KVL constraint given in eq. (3.21) can be simplified to

$$7973\left(\frac{N_t}{750}\right)^2 - \sum_{j=1}^{13} L_{pj} r_j Q_j^2(t) = 0, \text{ for } p = 1 \ldots 5, \tag{4.8}$$

where r_j is the branch resistance (see table 4.6), and L_{pj} is the path matrix given by

$$L = \begin{bmatrix} 1 & 1 & 0 & 0 & 0 & 1 & 0 & 0 & 0 & 0 & 1 & 0 & 1 \\ 1 & 1 & 0 & 1 & 0 & 0 & 1 & 0 & 0 & 1 & 0 & 1 & 1 \\ 1 & 1 & 0 & 0 & 0 & 1 & 0 & 0 & 1 & 1 & 0 & 1 & 1 \\ 1 & 0 & 1 & 0 & 0 & 0 & 0 & 1 & 0 & 0 & 0 & 1 & 1 \\ 1 & 0 & 1 & 0 & 1 & 0 & 1 & 0 & 0 & 1 & 0 & 1 & 1 \end{bmatrix}.$$

According to the nature of the problem, the *fmincon* solver in Matlab's optimization toolbox is used to solve for the optimal solution. The implemented code can be found in Appendix A.2.

4.5 LOAD MANAGEMENT

The load management study is essentially treated as an optimal scheduling problem. Hence, the optimal starting time of this cycle needs to be found that will result in minimum energy

cost according to the TOU tariff. As shown in table 4.1, there are 4 tasks which follow each other. Tasks 1,2,3, and 4 represent drilling, explosive charge-up, blasting, and cleaning, respectively.

Since the optimal staring time is the variable of interest, the magnitudes of the power consumption, associated with each task (P_1 to P_4) are actually irrelevant. As long as the magnitude of the power, associated with each task, is proportional to the flow rate requirement of the task, the optimal starting time will be the same. E.g. arbitrarily choosing $P_1 = 15.2W$, $P_2 = 10.3W$, $P_3 = 1W$ and $P_4 = 25.5W$, will result in exactly the same solution for the starting time if $P_1 = 100W$, $P_2 = 67.8W$, $P_3 = 6.58W$ and $P_4 = 167.8W$ were chosen.

In veiw of the foregoing, the objective function given by eq. (3.22) can be simplified to

$$J = \sum_{i=t_s}^{t_s+8-1} 15.2C(i) + \sum_{i=t_s+8}^{t_s+11-1} 10.3C(i) + \sum_{i=t_s+11}^{t_s+17-1} 1C(i) + \sum_{i=t_s+17}^{t_s+24-1} 25.5C(i) \qquad (4.9)$$

where t_s is the starting time of the schedule, and the decision variable; $C(i)$ is the electricity cost according to the TOU tariff. It must be noted that the decision variable was constrained to be integer values between 1 and 24, because one day was taken as the optimization period with the sampling interval equal to 1 hour.

The problem was solved using the genetic algorithm (GA) solver in Matlab's optimization toolbox. The GA solver was used because of the integer constraint on the variable. It is found that the minimum cost over a 24 hour period is obtained when the cycle is started at 05:00. Further detail into the programming part can be found in Appendix A.2.4.

4.6 CHAPTER SUMMARY

The theory presented in the previous chapter was applied to a specific network and fan, in this chapter. This included finding the operating point equations using real data from literature. The optimization problem was solved with respect to a specific mining schedule and varying tariff structures.

CHAPTER 5

RESULTS

The results are presented in this section. Three different scenarios are simulated; and within each of these scenarios, three cases are compared with respect to the energy cost. This is described below.

- Activity in branch 7 on a weekday
  - Baseline
  - Energy efficiency
  - Energy efficiency and load management
- Activity in branches 7 and 8, on a weekday
  - Baseline
  - Energy efficiency
  - Energy efficiency and load management
- Activity in branch 7 and 8, on a Weekend
  - Baseline
  - Energy efficiency
  - Energy efficiency and load management

For all cases, a safety margin of 3 m^3/s is included on the lower limit of the flow rate rate constraint. This is done to cater for the sensitivities in the solution from the optimization model, and ensure that the actual flow rate is never less than the minimum required flow rate at any branch. Thus the results obtained are slightly conservative.

5.1 ACTIVITY IN ONE BRANCH FOR A WEEKDAY

In this section, it is assumed that there is activity taking place in branch 7 only. Thus the flow rate constraints are changing for branch 7 only. The rest of the branches have upper and lower boundaries that do not change with time.

5.1.1 Baseline

For the baseline case it is assumed that the fan is run at a constant speed throughout the day, and this speed is determined by the maximum flow rate demand. From table 4.1, it can be seen that the maximum flow rate demand is 25.2 m^3/s. A safety margin of 3 m^3/s is kept on the lower limit, and no limit is put on the upper limit. Thus the fan operates to maintain a flow rate of 28.5 m^3/s in branch 7 throughout the day. The VOD for this case is described by

$$Q_7(t) \geq 28.5 \quad \text{for} \quad 00:00 \leq t \leq 24:00. \tag{5.1}$$

The optimization problem (shown in section 4.4) was solved according to the VOD given by eq. (5.1). It was found that the lowest speed the fan could run, while achieving the VOD requirement, was at 263.2 RPM. The resulting flow rates throughout the network is shown in fig. 5.1. It can be seen that the minimum specified flow rate of 28.5 m^3/s is satisfied for branch 7. Thus if the fan is run at 263.2 RPM the whole day according to the high demand season, weekday tariff, the total cost of energy would be R 1 585. Accordingly, the total daily energy consumption can be calculated to be 1 863 kWh. Calculating the cost according to the low demand season leads to R 864.

The non-linear equality constraints were violated by an absolute maximum value of 2.59×10^{-8}.

The linear equality constraints were violated by an absolute maximum value of 0.3117.

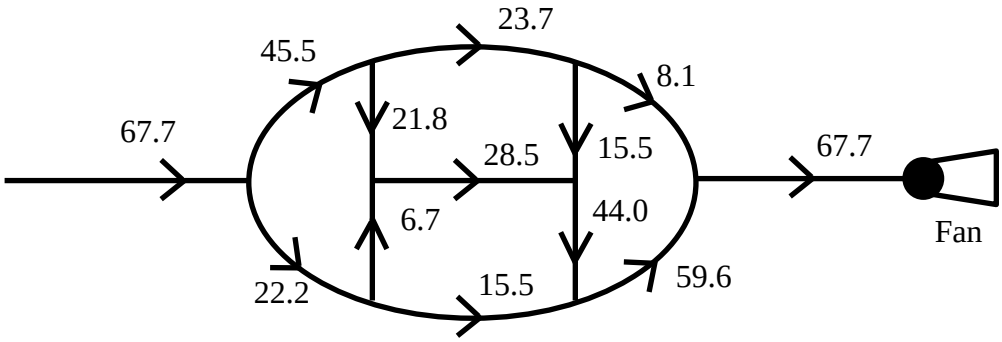

Figure 5.1: Constant flow rate of each branch in the network for the baseline case

5.1.2 Energy efficiency

In this section, the fan speeds are varied throughout the day, according to the VOD requirement. For this case, it is assumed that the cycle shown in table 4.1 is started at 00:00. Keeping a safety margin of 3 m^3/s, the VOD requirements are given as follows:

$$\begin{aligned} Q_7(t) &\geq 18.2 \quad \text{for} \quad 00:00 \leq t \leq 08:00, \\ Q_7(t) &\geq 13.3 \quad \text{for} \quad 08:00 \leq t \leq 11:00, \\ Q_7(t) &\geq 3.00 \quad \text{for} \quad 11:00 \leq t \leq 17:00, \\ Q_7(t) &\geq 28.5 \quad \text{for} \quad 17:00 \leq t \leq 24:00. \end{aligned} \tag{5.2}$$

The optimization problem shown in section 4.4 is solved, in accordance with the VOD requirements given by eq. (5.2). The results presented include the flow rate of branch 7 throughout the day, the optimal fan speed profile, and the power profile of the fan. They are presented in figs. 5.2, 5.3, and 5.4, respectively.

Fig. 5.3 shows that the fan speed is varied throughout the day, and this means that the power consumption will vary as well, reflected in fig. 5.4. The non-linear relationship is clearly visible, whereby dropping the speed from 168 RPM to 123 RPM reduces the power consumption from 20 kW to about 7.9 kW.

The optimized fan speed, during high demand season, results in a daily energy cost of R 695. Comparing this to a situation where the fan needs to be run at full capacity at all times to supply the maximum flow rate of 28.5 m^3/s to branch 7, a cost saving of R 890 per weekday

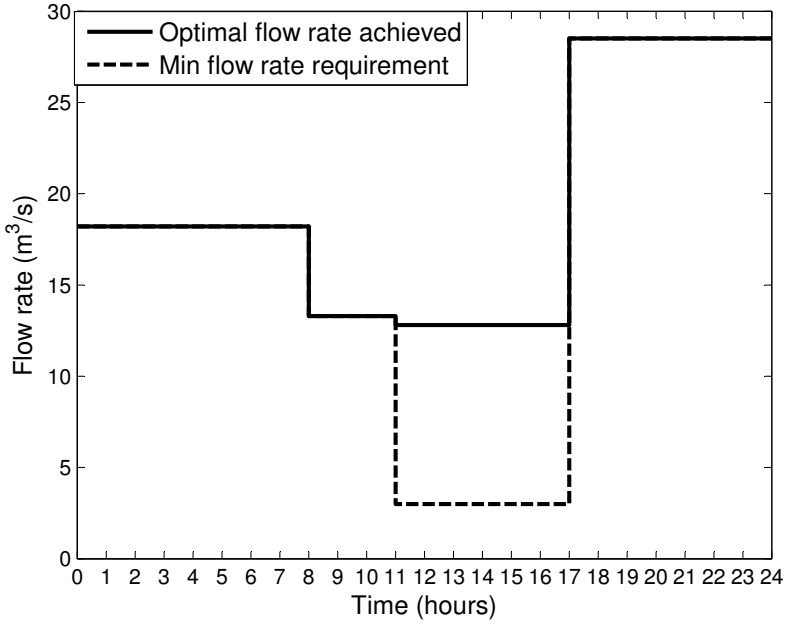

Figure 5.2: Flow rate in branch 7 for EE intervention only, for a weekday

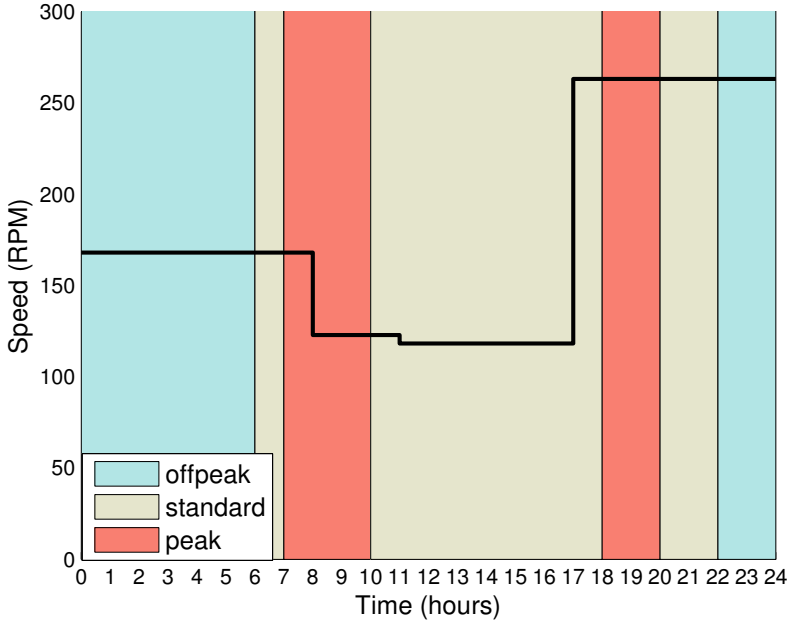

Figure 5.3: Optimal fan speed profile for EE intervention only, for a weekday

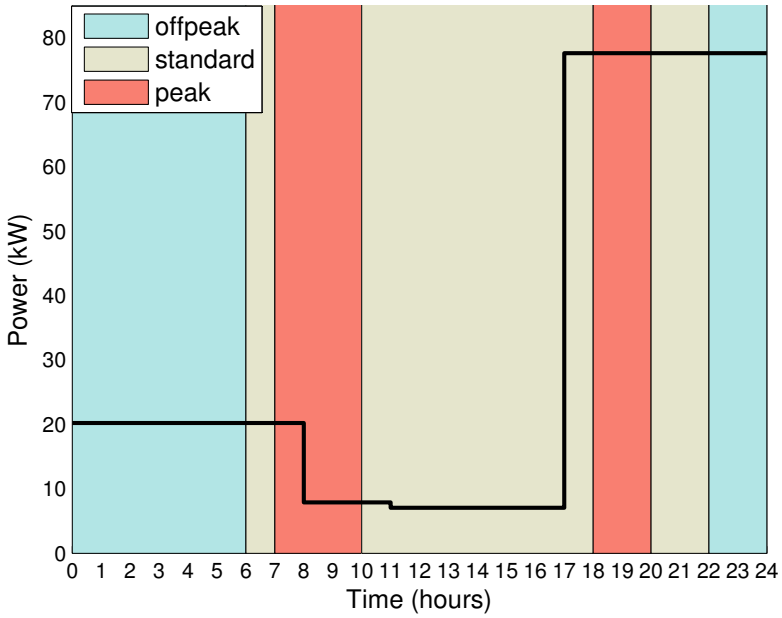

Figure 5.4: Power consumption of main fan for EE intervention only, for a weekday

is achieved. During low demand season, the energy cost after performing EE is R 361. This leads to a saving of R 503 per weekday.

In terms of energy savings, keeping a constant speed leads to daily energy consumption of 1 863 kWh; whereas varying the speed results in the daily consumption to be 771 kWh. This leads to daily savings of 1 092 kWh.

5.1.3 EE and LM

In section 5.1.2, the optimal fan speed profile was found, with the assumption that the mining cycle shown in table 4.1 was started at the beginning of the day, i.e., at 00:00. In this section, the optimal starting time is first found, based on the weekday tariffs for high and low season demand. This gives a new set of VOD requirements. The optimization problem shown in section 4.5 is solved, which results in the optimal starting time to be 05:00. Thus if the cycle is started at 05:00 and the constant safety margin of 3 m^3/s is kept, the new VOD

requirements are given by

$$\begin{aligned} Q_7(t) &\geq 18.2 \quad \text{for} \quad 05:00 \leq t \leq 13:00, \\ Q_7(t) &\geq 13.3 \quad \text{for} \quad 13:00 \leq t \leq 16:00, \\ Q_7(t) &\geq 3.00 \quad \text{for} \quad 16:00 \leq t \leq 22:00, \\ Q_7(t) &\geq 28.5 \quad \text{for} \quad 22:00 \leq t \leq 05:00. \end{aligned} \tag{5.3}$$

Thereafter, the procedure shown in section 4.4 is again followed, this time in accordance to the VOD requirements given by eq. (5.3). The results are presented in figs. 5.5, 5.6 and 5.7.

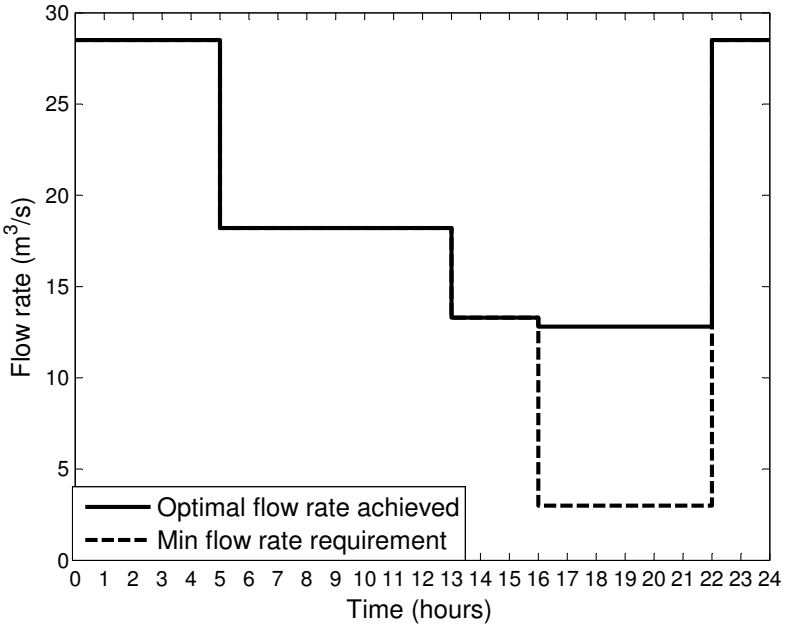

Figure 5.5: Flow rate in branch 7 for EE & LM, for a weekday

If the optimal speed profile is followed, during high demand season, the energy cost results to R 439. This leads to R 1 146 saving compared to the baseline case; and compared to EE case, a further R 256 saving per weekday. During low demand season, a saving of R 580 is achieved compared to the baseline case.

The non-linear equality constraints were violated by an absolute maximum value of 5.23×10^{-12}.

The linear equality constraints were violated by an absolute maximum value of 0.311.

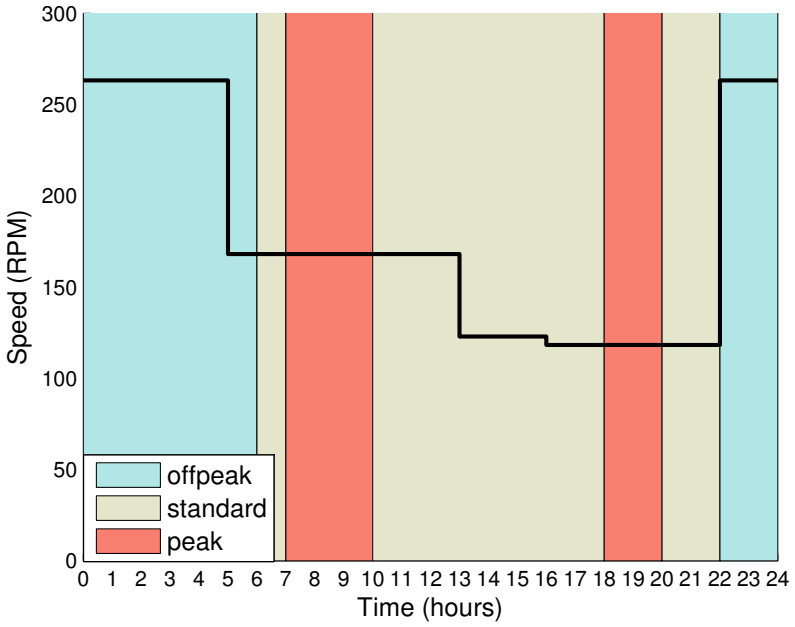

Figure 5.6: Optimal fan speed for EE & LM, for a weekday

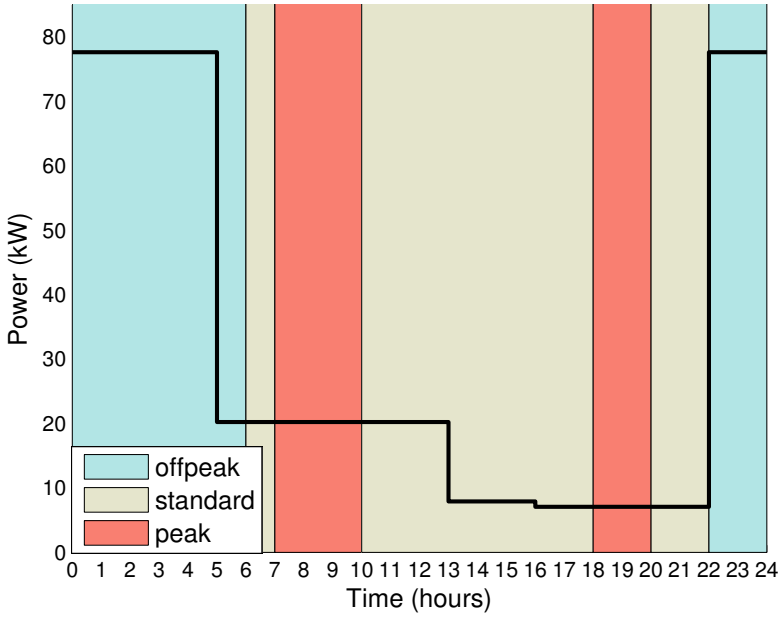

Figure 5.7: Power consumption of main fan for EE & LM, for a weekday

5.2 ACTIVITY IN TWO BRANCHES FOR A WEEKDAY

In this section, it is assumed that there is activity taking place in branches 7 and 8. Thus the VOD requirements are exactly the same as in section 5.1.1 with the addition that branch 8 must also follow the same ventilation pattern.

5.2.1 Baseline

The fan operates to maintain a flow rate of 28.5 m^3/s in branches 7 and 8 throughout the day. The VOD for this case is described by

$$Q_{7\&8}(t) \geq 28.5 \quad \text{for} \quad 00:00 \leq t \leq 24:00. \tag{5.4}$$

By solving the problem in the same way as in section 5.1.1, it was found that the lowest speed the fan could run, while achieving the VOD requirement, was at 482.8 RPM. The resulting flow rates throughout the network is shown in fig. 5.8. Accordingly, during high demand season, the total cost of energy would be R 9 781. The total daily energy consumption can be calculated to be 11 499 kWh. During low demand season, the cost of energy would be R 5 333 per weekday.

The non-linear equality constraints were violated by an absolute maximum value of 3.2×10^{-5}.

The linear equality constraints were violated by an absolute maximum value of 0.5717.

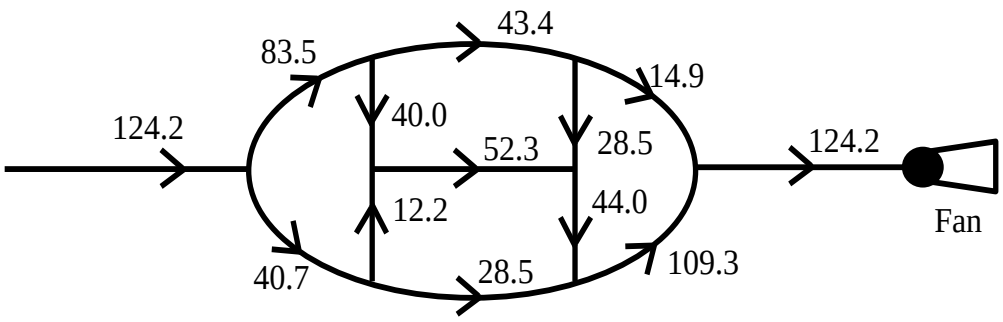

Figure 5.8: Constant Flow rate of each branch in the network for the baseline case

5.2.2 Energy efficiency

The fan speed is adjusted according to the VOD requirements given by

$$\begin{aligned} Q_{7\&8}(t) &\geq 18.2 \quad \text{for} \quad 00:00 \leq t \leq 08:00, \\ Q_{7\&8}(t) &\geq 13.3 \quad \text{for} \quad 08:00 \leq t \leq 11:00, \\ Q_{7\&8}(t) &\geq 3.00 \quad \text{for} \quad 11:00 \leq t \leq 17:00, \\ Q_{7\&8}(t) &\geq 28.5 \quad \text{for} \quad 17:00 \leq t \leq 24:00. \end{aligned} \tag{5.5}$$

The optimization problem is solved, similar to section 5.1.2. The results presented include the flow rates of branches 7 and 8 throughout the day, the optimal fan speed profile, and the power profile of the fan. They are presented in figs. 5.9, 5.10, 5.11, and 5.12, respectively.

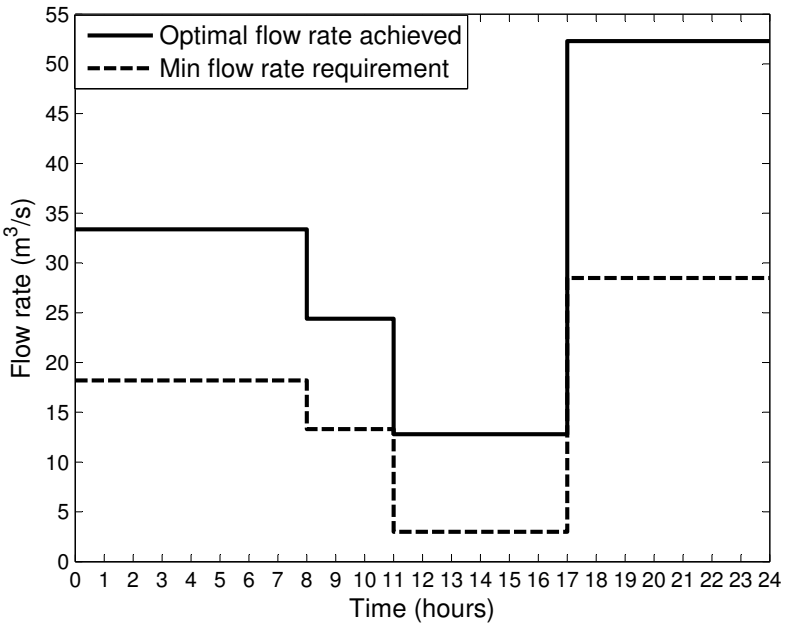

Figure 5.9: Flow rate in branch 7 for EE intervention only, for a weekday

The optimized fan speed, during high demand season, results in a daily energy cost of R 4 151. Comparing this to a situation where the fan needs to supply the maximum flow rate of 28.5 m^3/s to branches 7 and 8, leads to a cost saving of R 5 630 per Weekday. During low demand season the cost is R 2 120, which leads to a saving of R 3 213 per weekday.

In terms of energy savings, keeping a constant speed leads to daily energy consumption of 11 499 kWh; whereas varying the speed results in the daily consumption to be 4 540 kWh. This

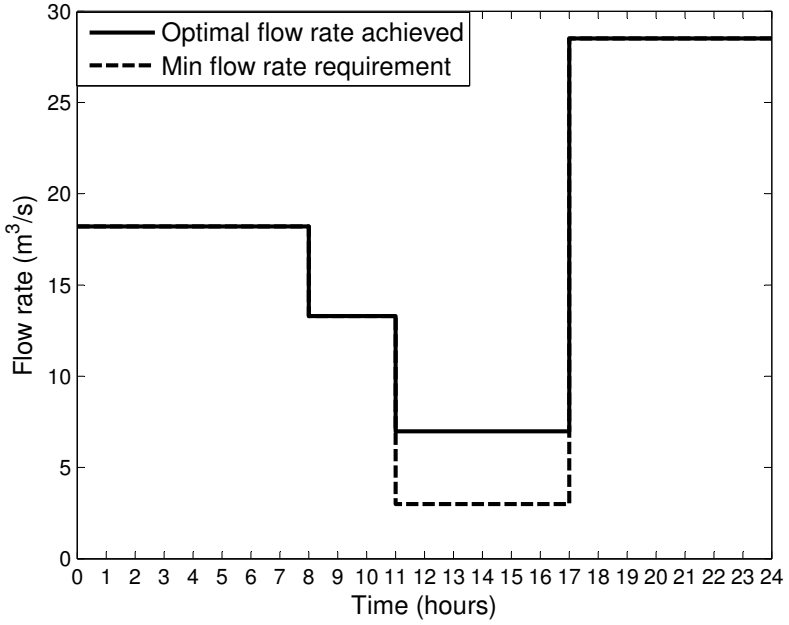

Figure 5.10: Flow rate in branch 8 for EE intervention only, for a weekday

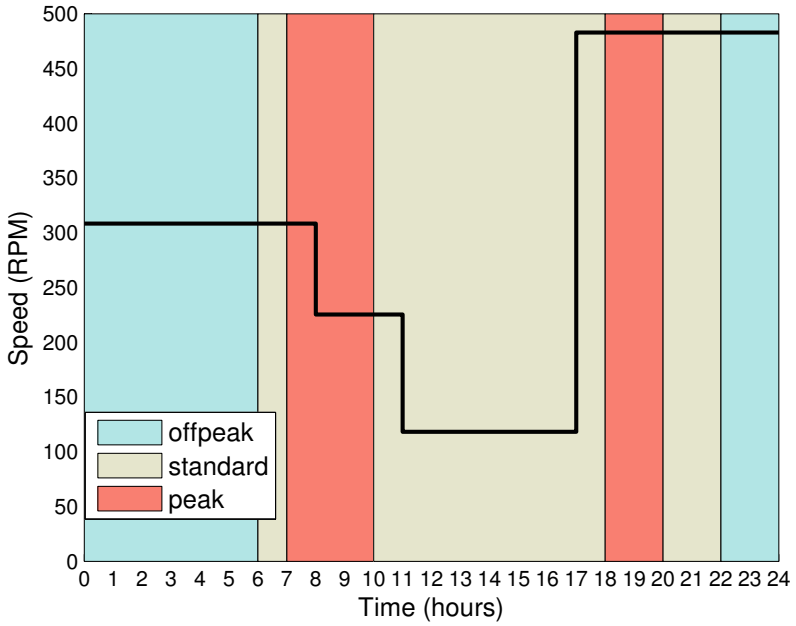

Figure 5.11: Optimal fan speed profile for EE intervention only, for a weekday

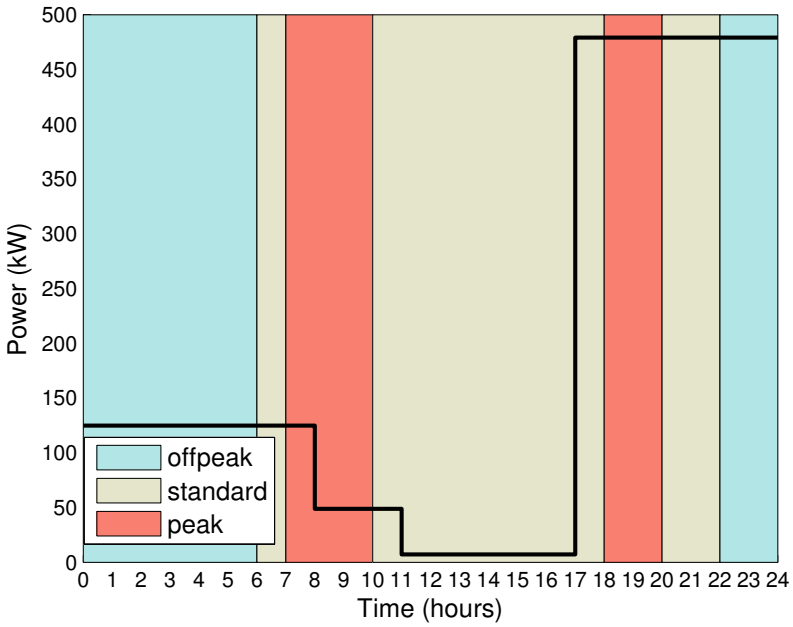

Figure 5.12: Power consumption of main fan for EE intervention only, for a weekday

leads to a daily saving of 6 959 kWh.

The non-linear equality constraints were violated by an absolute maximum value of 3.6×10^{-10}.

The linear equality constraints were violated by an absolute maximum value of 0.5717.

5.2.3 EE and LM

The number of active branches does not affect the optimal starting time, assuming they all follow the same schedule. Thus the cycle is started at 05:00 and the constant safety margin of 3 m^3/s is kept. The new VOD requirements are given by

$$\begin{aligned} Q_{7\&8}(t) &\geq 18.2 \quad \text{for} \quad 05:00 \leq t \leq 13:00, \\ Q_{7\&8}(t) &\geq 13.3 \quad \text{for} \quad 13:00 \leq t \leq 16:00, \\ Q_{7\&8}(t) &\geq 3.00 \quad \text{for} \quad 16:00 \leq t \leq 22:00, \\ Q_{7\&8}(t) &\geq 28.5 \quad \text{for} \quad 22:00 \leq t \leq 05:00. \end{aligned} \tag{5.6}$$

A similar process is followed as in section 5.1.3. The results are presented in figs. 5.13, 5.14, 5.15 and 5.16.

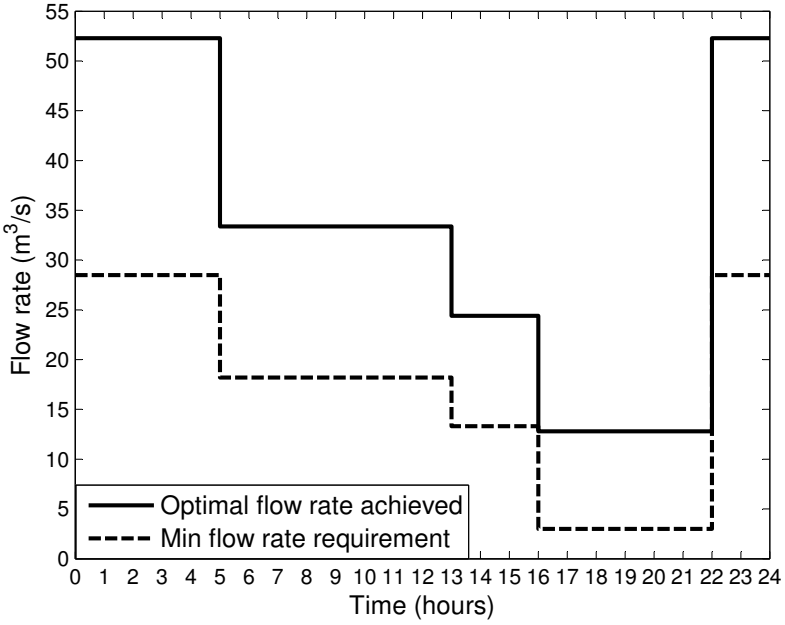

Figure 5.13: Flow rate in branch 7 for EE & LM, for a weekday

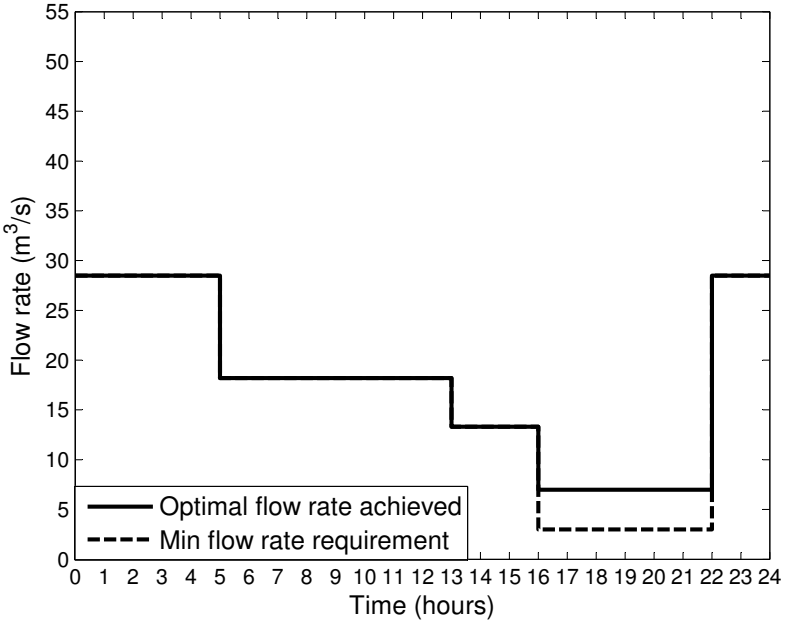

Figure 5.14: Flow rate in branch 8 for EE & LM, for a weekday

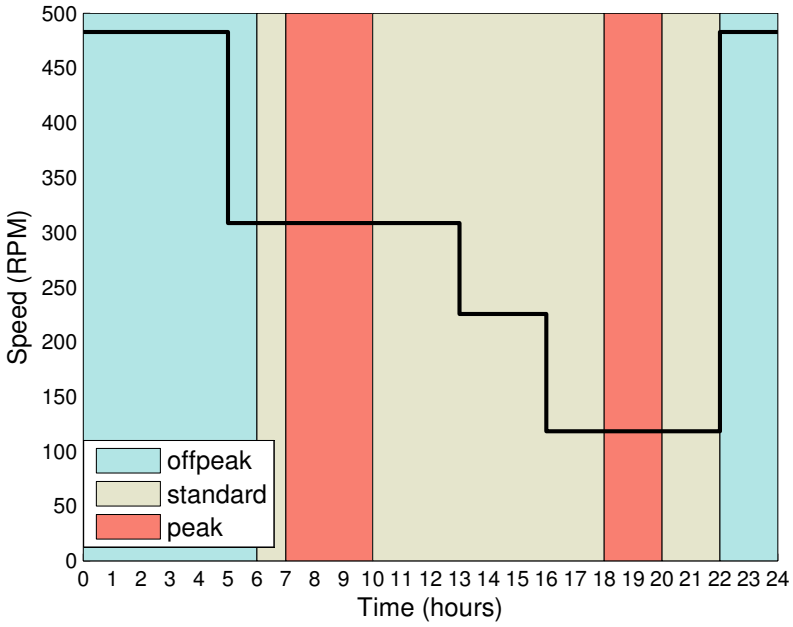

Figure 5.15: Optimal fan speed for EE & LM, for a weekday

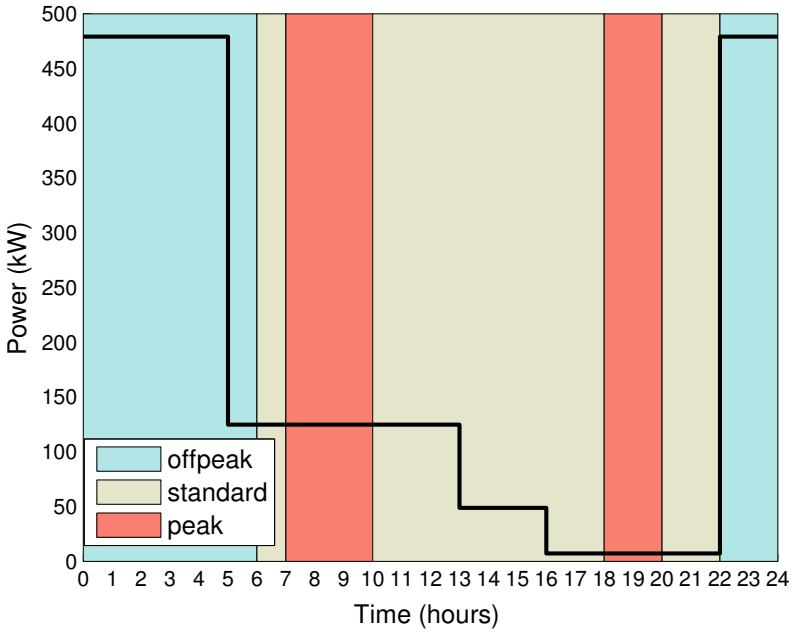

Figure 5.16: Power consumption of main fan for EE & LM, for a weekday

If the optimal speed profile is followed during a weekday in the high demand season, the energy cost results to R 2 464. This provides a R 7 317 saving compared to the baseline case, and a further R 1 687 saving compared to the EE case. During the low demand season, the energy cost would be R 1 635, leading to a saving of R 3 698, compared to the baseline case.

The non-linear equality constraints were violated by an absolute maximum value of 1.1×10^{-10}.

The linear equality constraints were violated by an absolute maximum value of 0.5717.

5.3 ACTIVITY IN TWO BRANCHES FOR A WEEKEND

This section presents the results of the case where activity is still taking place in branch 7 and 8, but a different tariff structure is used to calculate the energy costs.

5.3.1 Baseline

If the maximum demand of 28.5 m^3/s is maintained in branches 7 and 8 throughout the day, the VOD requirement is given by eq. (5.4). This problem is essentially the same as shown in section 5.2.1, except a different tariff structure is followed.

As expected, solving the problem leads to the same solution as section 5.2.1 of running the fan at 482.8 RPM. This leads to the same daily energy consumption of 11 499 kWh. The cost of energy on a Saturday and Sunday during high demand season is R 4 984 and R 4 002, respectively. During the low demand season, the costs are R 4 053 and R 3 450, respectively. The resultant flow rates through the network is also the same as given in fig. 5.8.

The non-linear equality constraints were violated by an absolute maximum value of 1.1×10^{-7}.

The linear equality constraints were violated by an absolute maximum value of 0.5717.

5.3.2 Energy efficiency

Again, most of the results of this section are the same as section 5.2.2, because only the tariff structure changes. Thus the VOD requirements are given by (5.5); the total energy consumption is still 4 540 kWh; the flow rates in branches 7 and 8, the the optimal fan speed profile, and the power profile of the fan still remain the same as given by figs. 5.9, 5.10, 5.11, and 5.12, respectively.

The only change is that the total cost of energy on a Saturday and Sunday during high demand season is R 1 942 and R 1 580, respectively. During the low demand season, the costs are R 1 585 and R 1 362, respectively.

Thus on a Saturday and Sunday, during high demand season, a saving of R 3 042 and R 2 422 is achieved, respectively. During low demand season, a similar analogy leads to a saving of R 2 468 and R 2 088, respectively.

The non-linear equality constraints were violated by an absolute maximum value of 4.5×10^{-12}.

The linear equality constraints were violated by an absolute maximum value of 0.5717.

5.3.3 EE and LM

Just like section 5.1.3 and 5.2.3, the optimal staring time of the mining cycle is found first. However, due to the change in the tariff structure that is followed, the optimal starting time was found to be at 19:00. This leads to a new set of VOD requirements for branch 7 and 8, given by

$$\begin{aligned} Q_{7\&8}(t) &\geq 18.2 \quad \text{for} \quad 19:00 \leq t \leq 03:00, \\ Q_{7\&8}(t) &\geq 13.3 \quad \text{for} \quad 03:00 \leq t \leq 06:00, \\ Q_{7\&8}(t) &\geq 3.00 \quad \text{for} \quad 06:00 \leq t \leq 12:00, \\ Q_{7\&8}(t) &\geq 28.5 \quad \text{for} \quad 12:00 \leq t \leq 19:00. \end{aligned} \tag{5.7}$$

The results are presented in figs. 5.17, 5.18, 5.19 and 5.20.

Following the optimal speed profile, on a Saturday during high demand, season leads to an

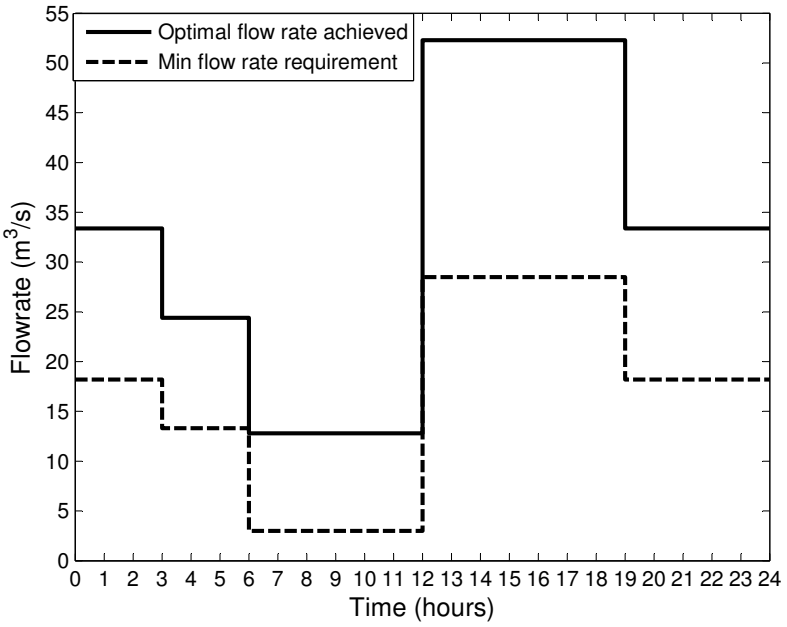

Figure 5.17: Flow rate in branch 7 for EE & LM, for a Saturday

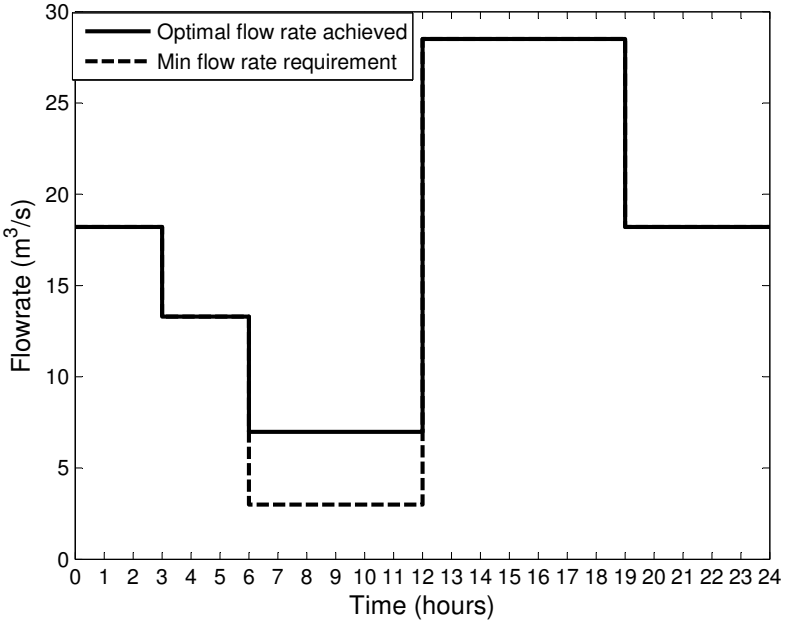

Figure 5.18: Flow rate in branch 8 for EE & LM, for a Saturday

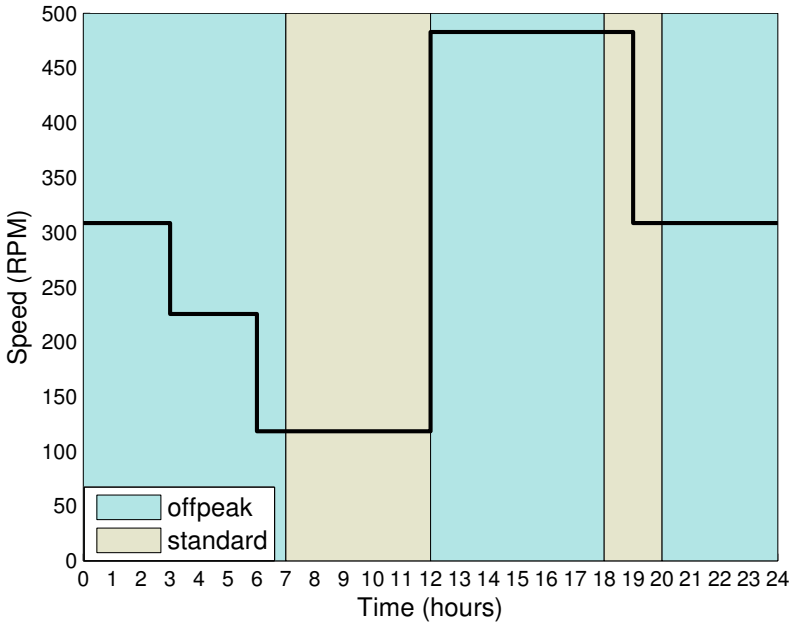

Figure 5.19: Optimal fan speed for EE & LM, for a Saturday

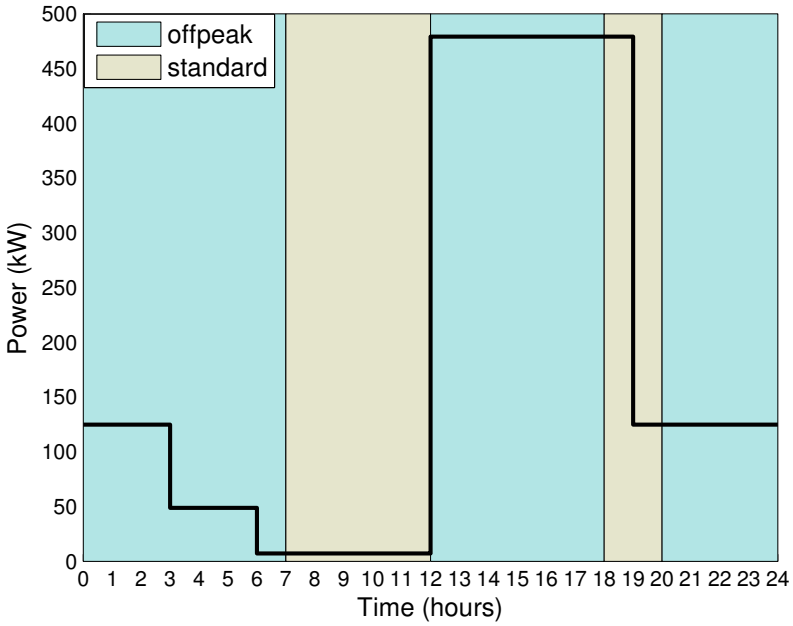

Figure 5.20: Power consumption of main fan for EE & LM, for a Saturday

energy cost of R 1 767. During the low demand season, the cost on a Saturday is R 1 477. Since the tariff on a Sunday is fixed throughout the day, there is no optimal starting time; i.e. starting any time on Sunday will lead to the same cost as the EE case.

Thus during high demand season on a Saturday, a saving of R 3 217 can be achieved, compared to the baseline case. During the low demand season, a saving of R 2 576 is achieved.

The total energy consumed remains the same, which is 4 540 kWh.

The non-linear equality constraints were violated by an absolute maximum value of 3.5×10^{-11}.

The linear equality constraints were violated by an absolute maximum value of 0.5717.

5.4 CHAPTER SUMMARY

The results of solving the optimization problems were shown in this chapter. A summary for the various cases during high and low demand season is shown in tables 5.1 and 5.2, respectively. The constraint violations are summarized in table 5.3. These results are discussed in chapter 6.

Table 5.1: Summary of results during high demand season. All values for a 24 hour period

Case		**1 branch weekday**	**2 branch weekday**	**2 branch Saturday**	**2 branch Sunday**
Baseline	Energy (kWh)	1 863	11 499	11 499	11 499
	Cost (R)	1 585	9 781	4 984	4 002
EE	Energy (kWh)	771	4 540	4 540	4 540
	Cost (R)	695	4 151	1 942	1 580
EE&LM	Energy (kWh)	771	4 540	4 540	4 540
	Cost (R)	439	2 464	1 767	1 580
Savings	Energy (kWh)	1 092	6 959	6 959	6 959
	EE (R)	890	5 630	3 042	2 422
	EE&LM (R)	1 146	7 317	3 217	2 422

Table 5.2: Summary of results during low demand season. All values for a 24 hour period

Case		1 branch weekday	2 branch weekday	2 branch Saturday	2 branch Sunday
Baseline	Energy (kWh)	1 863	11 499	11 499	11 499
	Cost (R)	864	5 333	4 053	3 450
EE	Energy (kWh)	771	4 540	4 540	4 540
	Cost (R)	361	2 120	1 585	1 362
EE&LM	Energy (kWh)	771	4 540	4 540	4 540
	Cost (R)	284	1 635	1 477	1 362
Savings	Energy (kWh)	1 092	6 959	6 959	6 959
	EE Cost (R)	503	3 213	2 468	2 088
	EE&LM Cost (R)	580	3 698	2 576	2 088

Table 5.3: Summary of constraint violations

Case		1 branch weekday	2 branch weekday	2 branch Sat & Sun
Baseline	Linear	0.3117	0.5717	0.5717
	Non-linear	2.17×10^{-6}	3.2×10^{-5}	1.1×10^{-7}
EE	Linear	0.3117	0.5717	0.5717
	Non-linear	6.8×10^{-10}	3.6×10^{-10}	4.6×10^{-6}
EE&LM	Linear	0.3117	0.5717	0.5717
	Non-linear	6.8×10^{-10}	1.1×10^{-10}	4.5×10^{-6}

CHAPTER 6

DISCUSSION

6.1 YEARLY SAVINGS & PAYBACK

Calculating the energy cost for a year (for the 2 branch baseline case) considers 52 weeks which consists of 5 weekdays, a Saturday, and a Sunday. It must also be noted that the high and low demand season is also considered in this calculation. Accordingly, the total cost leads to R 2 085 135. Based on a similar analogy, the total annual energy consumed for this case would be 4 185 636 kWh.

When only the EE activities are performed, the yearly energy cost and energy consumption is R 843 739 and 1 652 560 kWh, respectively. Thus compared to the baseline case, the annual cost savings and energy savings are R 1 241 396 (59.5%) and 2 533 076 kWh (60.5%), respectively.

When the LM activities are combined with the EE ones, the calculation of the number of days in a year is slightly different. In order to simplify the calculation, it is assumed that some hours are lost. The optimal starting time for a weekday, which is found to be at 05:00, is based only on the weekday tariff over a 24 hour period. The fact that the Friday schedule will run 5 hours into Saturday, might not make the solution optimal anymore. Similarly, the optimal Saturday starting time is found to be at 19:00. Thus the schedule, starting on Saturday at 19:00 will run 19 hours into Sunday, making the solution non-optimal. To avoid calculating the optimal times by using the whole year as the time horizon, it is assumed that a week consists of 4 weekdays and a Saturday, i.e. the Friday and Sunday are skipped from the savings calculations.

Based on the foregoing and assuming 52 weeks in a year, the adjusted baseline for 2 branches leads to an annual energy cost of R 1 563 419 and consumption of 2 989 740 kWh.

Accordingly, the annual cost and energy saving when considering EE & LM, compared to the adjusted baseline, is R 1 099 657 (70.3%) and 1 809 340 kWh (60.5%), respectively. As expected, the actual savings are less because 2 days are omitted from the calculations, but the percentage energy saving remains the same and the percentage cost saving is higher, when compared to the EE case.

In order to calculate the simple payback period of a VSD, the cost price is required. The findings from [30] suggest that the average cost of VSDs for fan applications is around $ 144/kW (R 1535/kWh). This would typically include the installation costs as well. Accordingly, the cost of a VSD would be $ 86 400 (R 921 024), assuming the fan used in this study is rated at 600 kW. This value also matches with prices procured from companies overseas. Thus, if the 1-branch EE case is implemented, the payback would be 4.8 years or about 57 months. If the 2-branch EE case is implemented, the payback period works out to be about 0.742 years or roughly 9 months. It can be seen that the number of active branches plays a major role in determining the payback. Both cases can be seen as viable according to [2], which says the payback should be less than one third of the motor life, which is assumed around 20 years. However, to meet the benchmark of a 2 year payback period (suggested in [30]), only the 2-branch case would be feasible. It can thus be concluded that the more active branches the main fan caters for, the shorter the payback for the VSD will be.

Another assumption which is made is that the fan runs 24 hours all year round, i.e. has a utilization factor of 100%. This assumption affects the payback period as well. In a working mine, the fan would probably not run continuously throughout the year, due to maintenance and other interruptions. However, even if the fan ran at 50% utilization factor, the 2-branch EE case would still have a payback of less than the 2 year benchmark.

6.2 EFFECT OF TARIFF

The effects of the tariff structure on the results were analyzed. It was found that the tariff structure had a significant influence on the cost saving. As expected, it had no effect on the energy savings, because this was dependent entirely on the VOD requirements.

Considering the high demand season, it can be calculated that the EE cost savings based on the weekday tariff results to 58%. When the EE & LM activities are combined, a cost saving of 74% is obtained.

The actual saving figures (in Rands) for the Saturday tariff is less than the weekday tariff; this is because the Saturday tariff is relatively cheaper, as there is no peak price. However, when analyzing the percentage savings compared to the baseline, it is found that a 61% EE cost saving, and 64% EE&LM cost saving is achieved.

It can be seen that following the Saturday tariff structure for the EE case leads to a slightly higher percentage saving compared to the weekday tariff. The point to note, however, is how the tariff structure affects the cost savings when the EE&LM cases are compared. When following the Saturday tariff, there is a significant drop in percentage saving, compared to when the weekday tariff is followed. This can be attributed to the fact that the lack of the peak price in the weekend tariff takes away the opportunity for large cost savings.

6.3 FLOW RATES ACHIEVED

The effect of the active branches on the achieved flow rates is discussed here.

For the baseline cases, it can be seen from fig. 5.1 that when only branch 7 is constrained to 28.5m^3/s, the achieved flow rate is equal to the lower bound. However when both branches, 7 and 8, are constrained, only branch 8 is able to match the lower bound of 28.5m^3/s; branch 7 has to maintain a flow rate of 52.3m^3/s, as shown in fig. 5.8.

In terms of the EE cases, a similar pattern is observed. It can be seen from fig. 5.2 that the flow rate achieved in branch 7 is equal to the lower bound for most part of the 24 hour period, whereas from figs. 5.9 and 5.10, it can be seen that when both branches are constrained, it is branch 8 that manages achieve a flow rate equal to the lower bound for most of the day, and branch 7 cannot achieve this. This observation is consistent through all the cases shown, including the EE and LM cases combined. The only difference is that that the higher demand is shifted to the off-peak and standard times, as shown in figs. 5.5, 5.13, 5.14, 5.17, and 5.18.

Further tests were conducted to verify whether the flow rate in branch 8 was responsible for

determining the flow rates through the other branches. These are not explicitly presented in the results section for the sake of redundancy. When only branch 8 was limited to a lower bound of 28.5 m^3/s, exactly the same solution was obtained as when branches 7 and 8 were bounded together, as in section 5.2.1. This result suggested that the flow rate in branch 8 was indeed responsible for the optimal solution, i.e. the fan speed and hence the total airflow quantity.

To determine why the flow rate of branch 8 is the determining factor, the network was simulated without considering the KVL constraints. Branches 7 and 8 were bounded to a lower limit of 20 m^3/s and 28.5 m^3/s, respectively. The results showed that while only the KCL constraints were considered, and the KVL constraints were not considered, it was possible for both branches to achieve these flow rates. This meant that the KCL constraints were not forcing branch 8 to be responsible for determining the flow rates through the other branches. This led to the hypothesis that it was the KVL constraints that determine the influential branches; in particular the resistance of the branches.

In this study, branch 8 has a considerably higher resistance than branch 7 (see table 4.6), and they both follow the same mining schedule (see table 4.1) meaning both their flow rates are bounded by the same lower limit. Logically, the pressure drop over branch 8 will be higher than branch 7 at any given point. The fan supply pressure must therefore maintain to match the highest pressure demand, which in this case is of branch 8. Thus branch 8 manages to achieve a flow rate equal to the lower bound, most of the time. The only time branch 8 will achieve flow rates higher than the lower bound is when it is physically limited by lower bounds in the other branches, as illustrated in figs 5.10 and 5.14.

In a network with one fan, the pressure drop of the fan must be equal to the pressure drops over each path because it forms part of every path. Hence in general, it can be concluded that it is the path with the highest pressure drop that will determine the pressure drop over of the fan, and hence the optimal fan speed. This is also in line with the longest path theory presented in [37].

6.4 VIOLATION OF CONSTRAINTS

From table 5.3, it can be seen that the highest value to violate the non-linear constraints is 3.2×10^{-5}. A '0' value would indicate that the solution adheres to this constraint perfectly. However since a non-zero value is obtained, it is important to understand how this affects the solution. The non-linear constraint is formed to satisfy the KVL equations given by eq. (4.8), which says that the pressure drop over the fan must be equal to the sum of pressure drops of each branch in the path. Thus a non-zero value for this constraint indicates that the pressure developed by the fan does not match the pressure losses in the path. Effectively, this means that the actual flow rates may not be equal to the optimal solution indicated by the model, when the fan is run at the optimal speed. To judge whether the solution obtained is acceptable, a simple analysis was performed, as discussed below.

To test the effect of the constraint violation, the example from fig. 3.3 in section 3.6 is used. The same conditions are applied and accordingly, the optimal simulation results are shown in table 3.1. The following procedure is followed:

1. The pressure loss of each path is calculated using the the obtained simulation results. Each path is calculated to have a pressure loss of 147.5 Pa.

2. If the non-linear constraint violation is as large as '0.1', it means the pressure loss over the path can be 147.5 ± 0.1.

3. Thus the question is what will be the values of the flow rates, based on altered value of the pressure loss. The flow rates can be found by solving a set of simultaneous equations based on KCL and KVL.

4. It was found that the flow rates differed from the simulated solutions by a maximum of 1%.

Intuitively it is assumed that the effect of the non-linear constraint violations on the actual flow rates is dependent on the network. However, this analysis shows that if the violations are within the order of 10^{-4} and smaller, the effect is quite minimal and the actual flow rates is well within the safety margin of 3 m^3/s put on the lower bounds. Hence, the results from the model can be seen as acceptable.

Similarly, the highest value to violate the linear constraints was 0.5717. Upon further investigation it was found that the violation was specifically caused by the linear equality constraint, given by eq. (4.6). This value being non-zero means that the actual flow rate in branch 13 can differ from the solution obtained (due to the resultant fan speed) by a maximum of 0.5717 m^3/s. However, given that a safety margin of 3 m^3/s was included in the lower bound of the flow rates, a difference of 0.5717 m^3/s does not violate the minimum stipulated requirement on the active branches. Thus the results presented can be seen as acceptable.

The constraints were also analyzed according to the varying cases. It is noticed that the linear constraint violation stays constant along with the number of active branches. After investigating the individual linear constraints for each case, it was found that the largest linear constraint violation was determined by the highest fan speed. Thus a higher fan speed can result in a higher mismatch between the solution flow rate and the actual flow rate, which results in a larger linear constraint violation. This is also evident from the fact that the linear constraint violation in the 2 branch case is higher than that of the 1 branch case. This is because activity in 2 branches will require the fan to run at higher speeds, compared to demand in 1 branch only. Thus a higher number of active branches will also result in larger constraint violations.

The non-linear constraint violations are much smaller in magnitude compared to the violation of the linear constraints. As such, it is difficult to spot any trend just from the cases shown in table 5.3. Thus eq. (4.8) was investigated for each path, and it was found that the constraint violations differ between different cases, even if the solution at some time is the same. An example is given below.

1. For the 1-branch baseline case, the constraint violations for each of the 5 paths for the first time instant are: 1.9×10^{-7}, 7.5×10^{-8}, 1.0×10^{-7}, 1.1×10^{-7}, and 2.2×10^{-6}.

2. For the 1-branch EE case, a similar requirement of 28.5 m^3/s in branch 7 occurs at 17:00. Thus the violations at 17:00 are: 1.4×10^{-11}, 5.2×10^{-11}, 2.3×10^{-11}, 6.7×10^{-12}, and 1.9×10^{-11}.

3. A requirement of 28.5 m^3/s also occurs at 18:00, for the 1-branch EE case. Thus the violations at 18:00 are: 6.9×10^{-12}, 3.1×10^{-12}, 1.4×10^{-12}, 5.2×10^{-12}, and 1.9×10^{-12}.

It can be seen from the 3 examples above that even at the same requirement of 28.5 m^3/s, the constraint violations for each path is different for the different cases. This leads to the conclusion that the model doesn't actually manage to select the exact same solution at every run, but they are very close to each other. Thus the number of active branches and the flow rate requirements doesn't have much effect on the non-linear constraints.

6.5 CHAPTER SUMMARY

The results presented in the previous chapter were analyzed and discussed, in this chapter. Calculating the payback period according to the varying scenarios showed that, in most cases, it is less than the benchmark of two years. Performing load management during a weekday was found to be more profitable. A larger number of active branches was found to be more beneficial for a network with one main fan. Finally the constraint violations were analyzed; they were found to be small enough, such that the optimal solutions obtained could be regarded as acceptable.

CHAPTER 7

CONCLUSION AND RECOMMENDATIONS

7.1 CONCLUSION

This study presented a non-linear, constrained, optimization model for an underground mining ventilation network. The model aimed to find the maximum possible energy savings, by adjusting the speed of the main fan according to the time varying demand for airflow. Furthermore, an optimal scheduling problem was also formulated, which was used to determine the maximum possible energy-cost saving. These two studies were termed the EE and EE&LM studies, respectively. These studies were evaluated for various scenarios, from which the following can be observed:

- All energy savings are achieved only as a result of varying the fan speed. The energy savings are heavily dependent on the VOD requirements, i.e. the variation in airflow requirements, and the time duration of each requirement. Therefore the savings will vary significantly for individual cases. For this particular study, a maximum of 60.5% energy saving can be achieved. Other VOD studies, which only consider application to auxiliary fans, achieve savings roughly between 30% and 50%. Thus application of VSDs to a main fan may prove to be more beneficial than just being limited to auxiliary fans.

- Cost saving is achieved as a result of EE and LM. The contribution towards cost saving, in a EE&LM case, is mainly due to the EE measures. That is, majority of the cost saving is achieved due to the fan consuming less power, compared to the mining activities being shifted out of peak times. This can be attributed to the cubic relationship between

power and fan speed, vs. a linear relation between power and the TOU tariff.

- When considering the cost saving due to load shifting, a higher variation between the prices of a tariff will lead to greater savings. That is, a tariff with a larger difference in price between the peak and off-peak time leads to large savings.

- Since one fan is controlling the airflow in all the airways, its lowest operating point is limited by the highest requirement within the network. Thus it is not possible to supply exactly the minimum requirement to every branch. Although this might be seen as inefficient or non-optimal, the benefit is seen when the number of branches that require a varying demand is increased.

- The simple payback period to install a VSD on the main fan, in a mine ventilation system, is also dependent on the specific case. In this study, a payback period of less than two years was found, which, from literature, seemed to be the benchmark for VSD applications.

In view of the foregoing, it can be concluded that there is significant potential for energy saving and energy-cost saving in mine ventilation networks. Particularly, the application of VSDs to main fans is shown to have merit.

7.2 RECOMMENDATION

Although the saving percentages may seem impressive, it is just an indication of the maximum possible savings and gives a foundation for further research. It should be noted that the size and complexity of the presented network is limited. Only an open loop environment is considered, which cannot cater for any disturbances in the mining branches. Also, the presence of additional main fans, booster fans, and leakage roadways would present further challenges to the model. As such, for further research, it is recommended that a closed loop system should be considered that can be solved using an optimal control approach. This study could also involve finding the optimal combination of booster, auxiliary, and main fan duties according to VOD. Another factor which could improve the accuracy of the model includes taking into account the efficiencies of the drives and motors. It is hoped that this research will be extended in a practical sense and will be applied to a mine, as a case study,

to determine the practical savings.

The model presented is not restricted to the mining environment. It could be applied to any problem which involves fluid dynamics and networks. This could include applications in other pipeline networks e.g. in manufacturing plants or municipality pumping stations. It could even be applied in more unrelated areas such as traffic flow optimization or in the field of wireless sensor networks.

REFERENCES

[1] C. Gellings, "The concept of demand-side management for electric utilities," *Proceedings of the IEEE*, vol. 73, no. 10, pp. 1468–1470, Oct. 1985.

[2] "A review on energy saving strategies in industrial sector," *Renewable and Sustainable Energy Reviews*, vol. 15, no. 1, pp. 150 – 168, Jan. 2011.

[3] Department of Energy, "Digest of South African energy statistics, 2009." [Online]. Available: http://www.energy.gov.za/files/media/explained/2009%20Digest%20PDF%20version.pdf

[4] G. Cheng, M. Qi, J. Zhang, W. Wang, and Y. Cheng, "Analysis of the stability of the ventilation system in baishan coalmine," *Procedia Engineering*, vol. 45, no. 0, pp. 311 – 316, 2012.

[5] D. O'Connor, "Ventilation on demand (VOD) auxiliary fan project - vale inco limited, creighton mine," in *proceedings of the 12th U.S./North American Mine Ventilation Symposium*, Nevada, June 2008, pp. 41–44.

[6] E. Acuña, S. Hall, S. Hardcastle, and L. Fava, "The application of a MIP model to select the optimum auxiliary fan and operational settings for multiple period duties," *INFOR*, Mar. 2010.

[7] S. Hardcastle, C. Kocsis, G. Li, and K. Hortin, "Analyzing ventilation requirements and the utilization efficiency of kidd creek mine ventilation system," in *Proceedings of the 12th U.S./North American Mine Ventilation Symposium*, Nevada, 2008, pp. 27–36.

[8] M. Medved, I. Ristovic, J. Roser, and M. Vulic, "An overview of two years of continuous

energy optimization at the velenje coal mine," *Energies*, June 2012.

[9] "Development and application of reservoir models and artificial neural networks for optimizing ventilation air requirements in development mining of coal seams," *International Journal of Coal Geology*, vol. 72, pp. 221 – 239, Feb. 2007.

[10] J. C. Kurnia, A. P. Sasmito, and A. S. Mujumdar, "Simulation of a novel intermittent ventilation system for underground mines," *Tunnelling and Underground Space Technology*, vol. 42, no. 0, pp. 206 – 215, May 2014.

[11] S. Saini, "Conservation v. generation: The significance of demand-side management (DSM), its tools and techniques," *Refocus*, vol. 5, no. 3, pp. 52 – 54, June 2004.

[12] G. Bellarmine, "Load management techniques," in *Southeastcon 2000. Proceedings of the IEEE*, April 2000, pp. 139–145.

[13] D. Loughran and J. Kulick, "Demand-side management and energy efficiency in the united states," *The Energy Journal*, vol. 25, no. 1, pp. 19–43, 2004.

[14] G. Wikler, A. Faruqui, C. Gellings, and K. Seiden, "The potential for energy efficiency in electric end use technologies," *Power Systems, IEEE Transactions on*, vol. 8, no. 3, pp. 1351–1357, Aug. 1993.

[15] P. Warren, "A review of demand-side management policy in the UK," *Renewable and Sustainable Energy Reviews*, vol. 29, no. 0, pp. 941 – 951, Jan. 2014.

[16] H. Nilsson, "The many faces of demand-side management," *Power Engineering Journal*, vol. 8, no. 5, pp. 207–210, Oct. 1994.

[17] Z. Paracha and P. Doulai, "Load management: techniques and methods in electric power system," in *Energy Management and Power Delivery, 1998. Proceedings of EMPD '98. 1998 International Conference on*, vol. 1, Mar. 1998, pp. 213–217.

[18] M. G. Patterson, "What is energy efficiency?: Concepts, indicators and methodological issues," *Energy Policy*, vol. 24, no. 5, pp. 377 – 390, May 1996.

[19] M. Eissa, "Demand side management program evaluation based on industrial and com-

mercial field data," *Energy Policy*, vol. 39, no. 10, pp. 5961 – 5969, Oct. 2011.

[20] A. Middelberg, J. Zhang, and X. Xia, "An optimal control model for load shifting Ű with application in the energy management of a colliery," *Applied Energy*, vol. 86, pp. 1266 – 1273, Aug. 2009.

[21] S. Zhang and X. Xia, "Optimal control of operation efficiency of belt conveyor systems," *Applied Energy*, vol. 87, no. 6, pp. 1929 – 1937, June 2010.

[22] A. J. van Staden, J. Zhang, and X. Xia, "A model predictive control strategy for load shifting in a water pumping scheme with maximum demand charges," *Applied Energy*, vol. 88, no. 12, pp. 4785 – 4794, Dec. 2011.

[23] Y. Tang, G. Zheng, and S. Zhang, "Optimal control approaches of pumping stations to achieve energy efficiency and load shifting," *International Journal of Electrical Power & Energy Systems*, vol. 55, no. 0, pp. 572 – 580, Feb. 2014.

[24] J. Zhang and X. Xia, "Best switching time of hot water cylinderŰswitched optimal control approach," in *Proceedings of the 8th IEEE AFRICON conference*, Namibia, Sept. 2007, pp. 1–7.

[25] S. Ashok, "Peak-load management in steel plants," *Applied Energy*, vol. 83, no. 5, pp. 413 – 424, May 2006.

[26] M. Teitel, A. Levi, Y. Zhao, M. Barak, E. Bar-lev, and D. Shmuel, "Energy saving in agricultural buildings through fan motor control by variable frequency drives," *Energy and Buildings*, vol. 40, no. 6, pp. 953 – 960, 2008.

[27] J. R. Eliason and B. S. Fisher, "Large adjustable speed fan drives including static converter developments for cement plants," *Industry Applications, IEEE Transactions on*, vol. IA-13, no. 6, pp. 557–562, Nov. 1977.

[28] I. Al-Bahadly, "Energy saving with variable speed drives in industry applications," in *Proceedings of the 2007 WSEAS Int. Conference on Circuits, Systems, Signal and Telecommunications*, Gold Coast Queensland, Jan. 2007, pp. 53–58.

[29] "Applications of variable speed drive (VSD) in electrical motors energy savings," *Renewable and Sustainable Energy Reviews*, vol. 16, no. 1, pp. 543 – 550, Jan. 2012.

[30] G. E. D. Plessis, L. Liebenberg, and E. H. Mathews, "The use of variable speed drives for cost-effective energy savings in south african mine cooling systems," *Applied Energy*, vol. 111, no. 0, pp. 16 – 27, Nov. 2013.

[31] E. Ozdemir, "Energy conservation opportunities with a variable speed controller in a boiler house," *Applied Thermal Engineering*, vol. 24, no. 7, pp. 981 – 993, May 2004.

[32] H. Zhang, X. Xia, and J. Zhang, "Optimal sizing and operation of pumping systems to achieve energy efficiency and load shifting," *Electric Power Systems Research*, vol. 86, no. 0, pp. 41 – 50, May 2012.

[33] R. Webber-Youngman, "An integrated approach towards the optimization of ventilation, air cooling and pumping requirements for hot mines," Ph.D. dissertation, North West University, Potchestroom, May 2005.

[34] C. Bise, *Modern American Coal Mining: Methods and Applications*, 1st ed. Society for Mining, Metallurgy, and Exploration, Inc., October 2013.

[35] J. M. A. Chadwick and M. Borthwick, *Hydraulic in Civil and Environmental Engineering*, 4th ed. Oxfordshire, England: Spon Press, 2004.

[36] J. Toraño, S. Torno, M. Menendez, M. Gent, and J. Velasco, "Models of methane behaviour in auxiliary ventilation of underground coal mining," *International Journal of Coal Geology*, vol. 80, no. 1, pp. 35 – 43, Oct. 2009.

[37] W. Hu and I. Longson, "The optimization of airflow distribution in ventilation networks using a nonlinear programming method," *Mining Science and Technology*, vol. 10, no. 2, pp. 209 – 219, Mar. 1990.

[38] B. Gay and P. Middleton, "The solution of pipe network problems," *Chemical Engineering Science*, vol. 26, no. 1, pp. 109 – 123, Jan 1971.

[39] C. Alexander and M. Sadiku, *Fundamentals of Electric Circuits*, 4th ed. McGraw-Hill,

August 2008.

[40] "An improvement of hardy cross method applied on looped spatial natural gas distribution networks," *Applied Energy*, vol. 86, pp. 1290 – 1300, Aug. 2009.

[41] S. Xiangyang and S. Yizhen, "Research on optimization algorithm wind quantity distribution in ventilation networks based on generic algorithm," in *Computational Intelligence and Natural Computing Proceedings (CINC), Second International Conference on*, vol. 1, Sept. 2010, pp. 154–158.

[42] J. Sui, L. Yang, Z. Zhu, H. Fang, and H. Zhen, "Mine ventilation optimization analysis and airflow control based on harmony annealing search," *Journal of Computers*, vol. 6, no. 6, pp. 1270–1277, June 2011.

[43] G. Wallace and O. Codoceo, "Ventilation planning at the el indio mine," in *Proceedings of the 6th International Mine Ventilation Congress*, May 1997, pp. 5–9.

[44] K. Wallace Jr., M. Tessier, M. Pahkala, and L. Sletmoen, "Optimization of the red lake mine ventilation system," in *Proceedings of the 11th U.S./North American Mine Ventilation Symposium*, Pennsylvania, 2006, pp. 61–66.

[45] S. Gillies, C. Slaughter, F. Calizaya, and W. Hsin, "Booster fans - some considerations for their usage in underground coal mines," in *Proceedings of the 13th U.S./North American Mine Ventilation Symposium*, 2010, pp. 511–518.

[46] I. Lowndes and Z. Yang, "The application of GA optimisation methods to the design of practical ventilation systems for multi-level metal mine operations," *Institution of Mining and Metallurgy. Transactions. Section A: Mining Technology*, vol. 113, no. 1, pp. A43–A57, Mar. 2004.

[47] C. Allen and B. Keen, "Ventilation on demand (VOD) project - vale inco ltd. coleman mine," in *proceedings of the 12th U.S./North American Mine Ventilation Symposium*, Nevada, June 2008, pp. 45–49.

[48] E. Bartsch, M. Laine, and M. Anderson, "The application and implementation of optimized mine ventilation on demand (OMVOD) at the Xstrata Nickel Rim South Mine,"

in *proceedings of the 13th U.S./North American Mine Ventilation Symposium*, Sudbury Ontario, June 2010, pp. 41–44.

[49] R. Papar, A. Szady, W. Huffer, V. Martin, and A. Mckane, "Increasing energy efficiency in mine ventilation systems," Lawrence Berkeley National Laboratory, University of California, Tech. Rep., 1999.

[50] H. Hartman, J. M. Mutmansky, R. V. Ramani, and Y. J. Wang, *Mine Ventilation and Air Conditioning*, 3rd ed. Wiley, November 1997.

[51] R. Carlson, "The correct method of calculating energy savings to justify adjustable frequency drives on pumps," in *Petroleum and Chemical Industry Conference. Industry Applications Society 46th Annual*, San Diego, Sept. 1999, pp. 275–283.

[52] G. Shim, L. Song, and G. Wang, "Comparison of different fan control strategies on a variable air volume systems through simulations and experiments," *Building and Environment*, vol. 72, no. 0, pp. 212 – 222, Feb. 2014.

APPENDIX A

MATLAB CODE

A.1 OPERATING POINT OF FAN

A.1.1 Flow to speed equation formulation

```
clc
clear all

Q = [200;225;250;275;300;325;350;375]; % flow rate points from fan
    curve

H = [7870;7730;7400;6730;6200;5600;5330;4000]; % pressure points
    from fan curve

S = [0.2122 0 0]; % system curve coefficients

h=polyfit(Q,H,2); % reproduce fan curve

% equating modified fan curve (according to fan laws) to system
    curve, and
% making flow rate 'Q' the subject of the formula. N=n/nfull.
E=solve('a2*Q^2 + a1*N*Q + a0*N^2 = s2*Q^2+s1*Q+s0','Q')

% substitute the variables with actual coefficients from the system
```

```
    curve
% and fan curve
f1=subs(E(2),'a2',h(1));
f2=subs(f1,'a1',h(2));
f3=subs(f2,'a0',h(3));
f4=subs(f3,'s2',S(1));
f5=subs(f4,'s1',S(2));
f6=subs(f5,'s0',S(3));

f7=simplify(f6)

% obtain function output values by inserting input values
q=@(x) subs(f7,'N',x);
t=1:5:2500;
q2=q(t);

% Fit a first order curve to the data obtained
q3=polyfit(t,q2,1); % flow, expressed as a function of relative
    speed
double(q3) % obtain the coeffiecients
```

A.1.2 Pressure to speed equation formulation

```
clc
clear all

Q = [200;225;250;275;300;325;350;375]; % flow rate points from fan
    curve

H = [7870;7730;7400;6730;6200;5600;5330;4000]; % pressure points
    from fan curve

S = [0.2122 0 0]; % system curve coefficients
```

```
9
10 h=polyfit(Q,H,2); % reproduce fan curve
11
12 % making 'Q' the subject of the modified (by the fan laws) fan
       curve equation
13 E1=solve('a2*Q^2 + a1*N*Q + a0*N^2==h','Q')
14
15 % making 'Q' the subject of the system curve equation
16 E2=solve('s2*Q^2+s0==h','Q')
17
18 % equate the 2 previous equations to get rid of 'Q'
19 E3=solve('-(N*a1 + (N^2*a1^2 - 4*a0*a2*N^2 + 4*a2*h)^(1/2))/(2*a2)
       ==(h - s0)^(1/2)/s2^(1/2)','h');
20
21 % substitute the variables with actual coefficients from the system
        curve
22 % and fan curve
23 f1=subs(E3(1),'a2',h(1));
24 f2=subs(f1,'a1',h(2));
25 f3=subs(f2,'a0',h(3));
26 f4=subs(f3,'s2',S(1));
27 f5=subs(f4,'s0',S(3));
28
29 f6=simplify(f5)
30
31 % obtain function output values by inserting input values
32 h2=@(x) subs(f6,'N',x);
33 t=1:5:2500;
34 h3=h2(t)
35
36 % Fit a second order curve to the data obtained
37 h4=polyfit(t,h3,2) % pressure, expressed as a function of relative
       speed
```

```
38 double(ps) % obtain the coeffiecients
```

A.1.3 Power to speed equation formulation

```
1  clc
2  clear all
3
4  Q = [200;225;250;275;300;325;350;375]; % flow rate points from fan
       curve
5
6  H = [7870;7730;7400;6730;6200;5600;5330;4000]; % pressure points
       from fan curve
7
8  P = [1833;1967;2067;2100;2133;2133;2167;2133]; % power points from
       fan power curve
9
10 S = [0.2122 0 0]; % system curve coefficients
11
12 h=polyfit(Q,H,2); % reproduce fan curve
13
14 p=polyfit(Q,P,3); % reproduce the power curve
15
16 % equating modified fan curve (according to fan laws) to system
       curve, and
17 % making flow rate 'Q' the subject of the formula. N=n/nfull.
18 E=solve('a2*Q^2 + a1*N*Q + a0*N^2 = s2*Q^2+s0','Q');
19
20 % Substituting the previous equation for 'Q' into the modified
       power
21 % equation.
22 E2=subs('e3*Q^3 + e2*N*Q^2 + e1*N^2*Q + e0*N^3','Q',E(1));
23
24 % substitute the variables with actual coefficients for the
```

```
    previous
% equation
p1=subs(E2,'a2',h(1));
p2=subs(p1,'a1',h(2));
p3=subs(p2,'a0',h(3));
p4=subs(p3,'s2',S(1));
p5=subs(p4,'s0',S(3));
p6=subs(p5,'e3',p(1));
p7=subs(p6,'e2',p(2));
p8=subs(p7,'e1',p(3));
p9=subs(p8,'e0',p(4));

p10=simplify(p9);

% obtain function output values by inserting input values
pr=@(x) subs(p10,'N',x);
t=1:5:250;
pr2=pr(t);

% Fit a third order curve to the data obtained
pr3=polyfit(t,pr2,3); % flow, expressed as a function of relative
    speed
double (pr3) % obtain the coeffiecients
```

A.2 OPTIMIZATION PROBLEMS

A.2.1 Objective

```
% objective function, takes in 'X' (which is a vector with all the
    fan speeds at all time intervals)
% and gives a scalar value 'y' (which is the total cost of
    electricity)

function y = objective(X)
```

```
%define global parameters

T = 24; % No of time intervals
K = 1; % No of fans

A =     1795.9/750^3; %coefficients of power vs. speed eqn
B = 0;                % All other coefficients assumed to be zero
C = 0;
D = 0;

% Defining the TOU tariff
peak=2.116;
off_peak=0.348;
standard=0.641;

for t=1:T
    if ((t>=1) && (t<=6))||((t>22)&&(t<=24))
        tou(t)=off_peak;
    elseif ((t>6) && (t<=7))||((t>10)&&(t<=18))||((t>20)&&(t<=22))
        tou(t)=standard;
    else tou(t)=peak;
    end
end

TOU=tou';
%%
g=1;
for k=1:K
    for t=1:T
        N(k,t)=X(g); % putting the variable 'N(k,t)' in one column
        g=g+1;
    end
end
```

```
%%
% formulate objective
sum = 0;
for k=1:K
    for t=1:T
        sum = sum + ((A*N(k,t)^3 + B*N(k,t)^2 + C*N(k,t) + D)*TOU(t
            ));
    end
end

y = sum


% A =    2245.1/750^3; %coefficients of power vs. speed eqn

% for t=1:T
```

A.2.2 Nonlinear constraints

```
%% Nonlinear constraint function. Takes in 'X' (all fan speeds and
    all flow rates at all time intervals). gives out nonlinear
    equality. nonlinear equality is left blank, as there is none.

function [c, ceq] = nonlincon (X)
r = [0.0225;0.1104;0.3;0.168;3.6;0.15;0.072;1.35;0.225;0.0551;4.5;
     0.0385;0.0585]  ; % branch resistance matrix

m = 9; %number of nodes
n = 13; %number of branches
T = 24; %number of time intervals
K = 1; %number of fans
b = n-m+1; %number of indepenent paths

```

```
13 L = [1 1 0 0 0 1 0 0 0 0 1 0 1; %path matrix
14       1 1 0 1 0 0 1 0 0 1 0 1 1;
15       1 1 0 0 0 1 0 0 1 1 0 1 1;
16       1 0 1 0 0 0 0 1 0 0 0 1 1;
17       1 0 1 0 1 0 1 0 0 1 0 1 1];
18
19 A = [0 0 0 0 0 0 0 0 0 0 0 0 1]; % 1 if thr is a fan 'k' in branch
       'j', otherwise 0
20
21 G=  7973.2/750^2; %coefficients for pressure vs. speed
22 I=0;
23 J=0;
24
25
26
27 %% Putting all the variables in one vector
28
29 g=1;
30 for k=1:K
31     for t=1:T
32         N(k,t)=X(g); % putting the variables 'N(k,t)' in one column
33         g=g+1;
34     end
35 end
36
37 h=g;
38 for j=1:n
39     for t=1:T
40         Q(j,t)=X(h); % putting the variables Q(j,t) in one column
41         h=h+1;
42     end
43 end
44
```

```
%% Nonlinear equality constraints (pressure drops=fan pressure)


for k=1:K
    for t=1:T
        H(k,t) = G*(N(k,t)^2) + I*(N(k,t)) + J; % expressing
            pressure drop over each fan as a function of speed
    end
end

i=1;
for t=1:T
    for p=1:b
        sum_path=0;
        for k=1:K
            for j=1:n
                sum_path=sum_path + ((L(p,j).*A(k,j).*H(k,t))
                                    - (L(p,j).*r(j).*(Q(j,t)^2))); %
                                        equality constraint - sum of
                                        pressure drop for each path
            end
        end
        ceq1(i) = sum_path;
        i=i+1;
    end
end

ceq=ceq1;
c=[];
```

A.2.3 Linear constraints

```
% Script to generate the Aeq and beq matrices for the optimization
```

```
    problem
clc
clear all

% Read the lb, ub, and x0 values for each control variable from an
    excel
% sheet.
lb=xlsread('lincon.xlsx','lb');
lb=lb';

ub=xlsread('lincon.xlsx','ub');
ub=ub';

x0=xlsread('lincon.xlsx','x0');
x0=x0';

% Associate each variable with a symbolic one at this stage
[X,txt]=xlsread('lincon.xlsx','syms');
X=txt;
X=sym(X);

E =  193.8399/750; % coefficients for flow vs. speed
F = 0;

m = 9; %number of nodes
n = 13; %number of branches
T = 24; %number of time intervals
K = 1; %number of fans

%%
A = [0 0 0 0 0 0 0 0 0 0 0 0 1]; % 1 if thr is a fan 'k' in branch
    'j', otherwise 0

```

```
B = [1 -1 -1  0  0  0  0  0  0  0  0  0  0; % Incidence matrix
     0  1  0 -1  0 -1  0  0  0  0  0  0  0;
     0  0  0  1  1  0 -1  0  0  0  0  0  0;
     0  0  1  0 -1  0  0 -1  0  0  0  0  0;
     0  0  0  0  0  1  0  0 -1  0 -1  0  0;
     0  0  0  0  0  0  1  0  1 -1  0  0  0;
     0  0  0  0  0  0  0  1  0  1  0 -1  0;
     0  0  0  0  0  0  0  0  0  0  1  1 -1;
    -1  0  0  0  0  0  0  0  0  0  0  0  1];

g=1;
for k=1:K
    for t=1:T
        N(k,t)=X(g); % putting the variables 'N(k,t)' in one column
        g=g+1;
    end
end

%% temp1: sum of flow at each node

h=g;
for j=1:n
    for t=1:T
        Q(j,t)=X(h); % putting the variables Q(j,t) in one column
        h=h+1;
    end
end

for t=1:T
    for i=1:m
        sum_node = 0;
        for j=1:n
            sum_node= sum_node + B(i,j).*Q(j,t); % equality
```

```
                constraint - sum of branches at each node
65          end
66          temp1(i,t) = sum_node;
67      end
68  end
69  %% temp2: flow of branch=flow of fan
70
71  for t=1:T
72      for k=1:K
73          sum = 0;
74          for j=1:n
75              if (A(k,j) == 1)
76                  sum= A(k,j).*-(E*N(k,t) + F)+Q(j,t); % flow of fan=
                        flow of branch
77              end
78          end
79          temp2(k,t) = sum;
80      end
81  end
82  %% temp: putting temp1 and temp2 together
83
84  for t=1:T
85      e=1;
86      f=1;
87      for d=1:(K+m)
88          if d<=m
89              temp(d,t)=temp1(e,t); % putting all equality
                    constraints in one column
90              e=e+1;
91          else
92              temp(d,t)=temp2(f,t);
93              f=f+1;
94          end
```

```
95      end
96  end
97  %% getting the matrix from the equations
98
99  l=1;
100 for d=1:(m+K)
101     for t=1:T
102         [a,b]=equationsToMatrix(temp(d,t),[X(1:(K*T+n*T))]);
103
104         Aeq(l,(1:(K*T+n*T)))= a(1,1:(K*T+n*T));
105         beq(l,1)=b;
106         l=l+1;
107     end
108
109 end
110
111 Aeq=double(Aeq);
112 beq=double(beq);
```

A.2.4 Optimal scheduling problem

```
1  %function that takes in the starting time as the input, and gives
       the
2  %cost of the schedule as the output.
3  function J = object(ts1)
4  % duration of each process in hours
5  tp1 = 8;
6  tp2 = 3;
7  tp3 = 6;
8  tp4 = 7;
9
10 % power associated with each process in hours
11 P1 = 3;
```

```
12 P2 = 2;
13 P3 = 1;
14 P4 = 4;
15
16 T = 24;
17 peak=2.116;
18 off_peak=0.348;
19 standard=0.641;
20
21 % Weekday tariff
22
23 % for t=1:T
24 %     if ((t>=1) && (t<=6))||((t>22)&&(t<=24))
25 %         tou(t)=off_peak;
26 %     elseif ((t>6) && (t<=7))||((t>10)&&(t<=18))||((t>20)&&(t<=22)
       )
27 %         tou(t)=standard;
28 %     else tou(t)=peak;
29 %     end
30 % end
31
32 %Weekend tariff
33 for t=1:T
34     if ((t>=1) && (t<=7))||((t>12)&&(t<=18))||((t>20)&&(t<=24))
35         tou(t)=off_peak;
36     else tou(t)=standard;
37     end
38 end
39
40 TOU=tou'
41
42 %%
43 % formulate objective
```

```
44
45 % Cost of process no. 1
46 sum1 = 0;
47 for i=ts1:ts1+tp1-1
48     if i>24
49         i=i-24;
50     end
51     sum1 = sum1 + (P1*(tou(i)));
52 end
53
54 % Cost of process no. 2
55 sum2 = 0;
56 for i=(ts1+tp1):(ts1+tp1+tp2-1)
57     if i>24
58         i=i-24;
59     end
60     sum2 = sum2 + (P2*(tou(i)));
61 end
62
63 % Cost of process no. 3
64 sum3 = 0;
65 for i=(ts1+tp1+tp2):(ts1+tp1+tp2+tp3-1)
66     if i>24
67         i=i-24;
68     end
69     sum3 = sum3 + (P3*(tou(i)));
70 end
71
72 % Cost of process no. 4
73 sum4 = 0;
74 for i=(ts1+tp1+tp2+tp3):(ts1+tp1+tp2+tp3+tp4-1)
75     if i>24
76         i=i-24;
```

```
77        end
78        sum4 = sum4 + (P4*(tou(i)));
79    end
80
81    % total cost of entire schedule
82    J = sum1+sum2+sum3+sum4;
83
84    end
```

A.2.5 Calling of optimization algorithms

```
1   clc
2   clear all
3
4   % Run fmincon for EE optimization
5   options = optimoptions('fmincon','Algorithm','SQP','TolCon',1e-4);
6   x=fmincon(@objective, x0,[],[],Aeq,beq,lb,ub,@nonlincon,options);
7
8   % Run ga for LS optimization
9   x0=1;
10  options=gaoptimset('InitialPopulation',x0);
11  x =  ga(@object,1,[],[],[],[],1,24,[],[1])
```